(1)

AD-A220 475

DTIC
ELECTE
APR 16 1990
S D
B

DEPARTMENT OF THE AIR FORCE

AIR UNIVERSITY

AIR FORCE INSTITUTE OF TECHNOLOGY

Wright-Patterson Air Force Base, Ohio

DISTRIBUTION STATEMENT A
Approved for public release;
Distribution Unlimited

90 04 13 212

(1)

AFIT/GA/ENY/90M-2

ANALYSIS OF THE USE OF A METHANE PROPELLANT IN A BIOWASTE RESISTOJET

THESIS

John A. Vise
Captain, USAF

AFIT/GA/ENY/90M-2

DTIC
ELECTE
APR 16 1990
S B D

Approved for public release; distribution unlimited

AFIT/GA/ENY/90M-2

ANALYSIS OF THE USE OF A METHANE PROPELLANT IN A BIOWASTE RESISTOJET

THESIS

Presented to the Faculty of the School of Engineering

of the Air Force Institute of Technology

Air University

In Partial Fulfillment of the

Requirements for the Degree of

Master of Science in Astronautical Engineering

John A. Vise, B.S.C.E.

Captain, USAF

QUALITY INSPECTED 1

Accession For
NTIS GRA&I ☑
DTIC TAB ☐
Unannounced ☐
Justification
By
Distribution/
Availability Codes
Dist | Avail and/or Special
A-1

March 1990

Approved for public release; distribution unlimited

Acknowledgements

I wish to thank Capt James Planeaux, my faculty advisor, and Capt Peter Haaland of the Department of Physics for their guidance and support throughout this investigation. I also wish to thank Dr. W. Earl Morren of the NASA Lewis Research Center, and LTC Tony Wachinski of the Department of Civil Engineering, US Air Force Academy, for their information and assistance.

Table of Contents

List of Figures

List of Tables

Notation

A_e	Nozzle exit area (m^2)
A_{pt}	Effective wall cross-sectional area (m^2)
$\bar{c}$	Mean molecular velocity (m/sec)
c_p	Specific heat at constant pressure (Nm/KgK)
CF	Specific impulse correction factor
D_h	Hydraulic diameter (m)
E	Activation energy for a reaction (cal/mole)
f	Fanning friction factor
F	Thrust (mN)
g_o	Gravitational constant = 9.81 m/sec^2
h	Convection heat transfer coefficient (W/m^2K)
h_c, h_e	Molecular enthalpy (kcal/mole)
I_s	Specific impulse (sec)
k	Kinetic rate constant (sec^{-1})
k_c	Thermal conductivity of carbon (W/mK)
k_f	Fluid thermal conductivity (W/mK)
k_{pt}	Thermal conductivity of platinum (W/mK)
$\dot{m}$	Mass flow rate (Kg/hr)
M	Molecular weight
Nu	Nusselt number
p	Pressure (atm)
P	Channel cross-section perimeter (m)
P_{CH_4}	Pressure of methane (atm)

q	Heat transfer rate (W)
q''	Heat flux (W/m^2)
r	Rate of methane conversion (mole/l sec)
r_d	Deposition rate ($\mu m/hr$)
R	Universal gas constant = 8.314 Nm/moleK
Re	Reynolds number
S°	Entropy (cal/moleK)
S_n	Number of heater sections
T_m	Heat exchanger fluid temperature (K)
T_s	Heat exchanger surface temperature (K)
u_m	Fluid mean velocity (m/sec)
V_e	Nozzle exit velocity (m/sec)
W	Resistojet operating power (W)
x_{fd}	Flow development length (cm)
Δx	Channel section length (cm)

Greek Notation

α	Molar fraction of depositing molecules
δ	Deposition thickness (μm)
ε	Mean kinetic energy (eV)
γ	Ratio of specific heats
Λ	Power scaling factor
μ	Viscosity ($Nsec/m^2$)
ρ	Density (Kg/m^3)
Γ	Flux of depositing molecules

Abstract

An engineering model resistojet has been developed by NASA for possible space station applications that will operate on a variety of waste gases, including methane. This investigation develops a computer program using the principles of laminar flow heat transfer to simulate operation of the resistojet heat exchanger. The principles of chemical kinetics are used to determine how carbon deposits from methane decomposition in the heat exchanger. The results of the program show a wide variation in deposition versus operational pressure, power, and methane mass flow rate.

I. Introduction

The US manned space station will require a method for low thrust propulsion to provide orbital maintenance and stationkeeping. NASA has developed an engineering model of a resistojet suitable for this purpose. The resistojet consists of a platinum heater surrounding a multichannel platinum heat exchanger that exits into a conical nozzle. The resistojet employs a variety of propellant fluids, including methane.

The purpose of this investigation is to construct a computer program to simulate the operation of the resistojet heat exchanger, using the principles of fluid mechanics and laminar flow heat transfer. The program will be adaptable to any proposed resistojet propellant, but is used in this study to examine operation with methane. The chemical kinetics of methane decomposition are used to determine the carbon deposition rate in the heat exchanger.

The program analyzes how carbon is deposited in the heat exchanger over time during steady operation, and how gas flow in the heat exchanger is affected by the deposition. The program is then run under a variety of methane operating conditions to show how carbon deposition varies with respect to gas pressure, operating power level, and propellant mass flow rate.

Results are presented in graphical format. Discussion of the results is extended to the resistojet nozzle, where carbon deposition will have the most impact on resistojet performance. A copy of the program is included for further studies.

II. Background

The US manned space station will have a variety of propulsion requirements throughout its operation. To meet these requirements, NASA has been conducting extensive research into several propulsion options for the station. When deployed, the space station will use both high and low thrust propulsion systems to meet its operational needs. Presently, NASA plans to provide high thrust (25-50 lb_f) from gaseous O_2/H_2 fueled rockets, and low thrust (50-100 mlb_f) from multipropellant resistojets (13:1).

The purpose of the space station resistojet is to provide small quantities of thrust over long periods of time for station attitude control and orbital maintenance. In this capacity the resistojet provides a supplement and back-up to the primary O_2/H_2 propulsion system for the station.

The resistojet is designed to operate with a variety of propellants. This versatility lets the resistojet employ waste fluids generated by the space station. By using waste gases as their propellants, the resistojets will not require additional fuel to be ferried up to the space station, and the waste products generated by the station will not have to be brought back to earth for disposal. Therefore, resistojets have the secondary advantage of reducing the overall operational cost for the space station (9:2).

Specifically, the resistojet developed by the Lewis Research Center was designed to meet several specific requirements (9:3-4):

1. Operate using the waste fluids most likely to be produced in significant quantities by the space station, including argon, carbon dioxide, helium, hydrogen, krypton, methane, nitrogen, oxygen, water, and cabin air. These gases will be produced by the station environmental system and by various experiments planned for the station.

2. Provide up to 110 mlb of thrust without exceeding a maximum power requirement of 2 KW.

3. Operate without scheduled maintenance for a 10 year mission with an operating life of at least 10,000 hours.

4. Provide for an ease of extra-vehicular deployment and servicing.

The space station is projected to eventually produce over 1800 Kg/year of waste fluids which would be available for propulsion. Methane would make up twenty per cent of this total, or about 350 Kg/year (13:5-9). Methane's relatively low molecular weight among the proposed resistojet propellants means it can achieve a higher

specific impulse than many of its alternatives. This high fuel efficiency makes methane an attractive candidate for resistojet propulsion.

Methane, however, has the disadvantage of decomposing at high temperatures, depositing solid carbon in the process. Over time, the build up of carbon could interfere with the performance of a resistojet, reducing its thrust and possibly requiring costly extra-vehicular maintenance.

Methane decomposition takes place in significant amounts only at relatively high temperatures, so the problem of carbon deposition can be avoided if the resistojet is operated at lower temperatures. Lower operating temperatures, though, mean lower thrust and specific impulse output from the resistojet, reducing the effectiveness of methane as a propellant. Determining the limiting operational temperatures and times of a resistojet with a methane propellant is then an important factor in maximizing the efficiency of the resistojet.

To meet these resistojet performance requirements, a model resistojet has been built and tested by NASA's Lewis Research Center (LRC). The model will demonstrate the viability of using space station waste fluids as propellants, as well as determining the specific fuel requirements for the low thrust propulsion system.

Resistojet Model Description

The engineering model multipropellant resistojet developed by LRC consists of a grain-stabilized platinum cylindrical heat exchanger inside a coiled sheathed heater, and a conical nozzle. The assembly of the resistojet is detailed extensively in other studies. (3:2-4; 18:197-198; 26:2-5). A cross-section of the resistojet is shown in Figure 2-1.

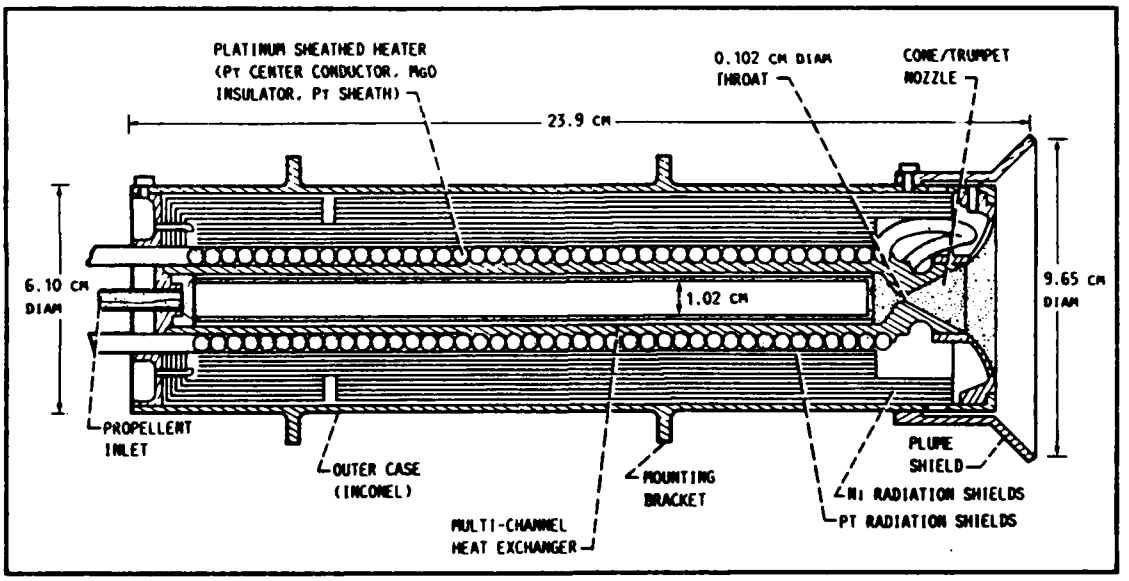

Figure 2-1. Engineering Model Resistojet (18:198)

The heat exchanger consists of a 10.2 cm long cylindrical shell with a series of semicircular grooves tooled on its outer surface, and 36 axial channels cut into its inner surface. The grooves are matched to the heater element and ensure the proper location of the heater relative to the heat exchanger, as well as provide a large surface area for the conduction of heat to the heat exchanger.

A hollow core cylinder inside the heat exchanger is flanged at the upstream end, forcing the propellant to flow through 36 1.27 mm x 0.5 mm channels between the core outer surface and the heat exchanger inner surface. At the downstream end, the channels end in a small chamber, where the propellant flow is merged prior to acceleration through the nozzle. A cross-section of a heat exchanger channel is shown in Figure 4-2.

Both the heat exchanger and the core were made from platinum grain-stabilized with less than 1 percent zirconium oxide dispersant. Platinum provides a heat exchanger surface that is compatible with a variety of gases, and thus can operate over long periods of time without material recession. Zirconium oxide provides grain stabilization and minimizes grain growth within the platinum, which can occur if the platinum is kept at a high temperature over a long period of time. Grain growth can weaken the components of the resistojet by causing voids, physical distortions, and

stress performance reductions in the platinum (32:1). Without grain stabilization, then, the life span of a resistojet would be severely restricted.

The resistojet heater was constructed from a 1.56 mm diameter platinum/10% rhodium conductor surrounded by a layer of magnesium oxide insulator. The heater unit is contained within a grain-stabilized platinum sheath. The heater is folded in half and wound in a double helix configuration. The heater is wrapped by a grain-stabilized platinum ribbon, and is surrounded by a radiation shield consisting of three layers of platinum foil, and seven layers of nickel foil, all separated by a small diameter wire. This assembly is then contained within a support shroud to protect the heat exchanger and provide a means for mounting the resistojet.

The nozzle is also made from grain-stabilized platinum. Propellant from the 36 channels of the heat exchanger is merged and accelerated through a 1.016 mm diameter throat. The expansion section diverges at a 25° half angle to an area ratio of 225/1. A trumpet extension to the conical nozzle increases the area ratio to 2500/1. The nozzle is also surrounded by a plume shield. The nozzle geometry was designed to minimize the impact of the resistojet plume to instrumentation aboard the space station, and to observations by equipment from the space station (4:1-2).

III. Methane Decomposition

The decomposition of methane is a complex process involving several intermediate species. The process starts with the production of ethane, and forms many different hydrocarbon species. Deposited carbon is but one of these methane products, but it is this deposition which can impact the performance of a resistojet.

The successive stages of carbon formation from methane are as follows (15:253-263):

$$2CH_4 \rightarrow C_2H_6 + H_2 \rightarrow C_2H_4 + 2H_2 \rightarrow C_2H_2 + 3H_2 \rightarrow 2C_{(s)} + 4H_2 \qquad (3\text{-}1)$$

Methane to Ethane

The first step of methane decomposition is the conversion of methane to ethane via a reaction series forming C_2H_6 through the formation of a methyl radical (CH_3) (21:348-353):

The exact mechanism for the conversion of methane to ethane may proceed by either of two different reaction mechanisms. One involves reactions with the methyl radical only (21:351-352):

$$CH_4 \rightarrow CH_3 + H \qquad (3\text{-}2)$$

$$CH_3 + CH_4 \rightarrow C_2H_6 + H \qquad (3\text{-}3)$$

The second reaction mechanism also involves the methylene radical (CH_2) as an intermediate species (15:261):

$$CH_4 \rightarrow CH_2 + H_2 \qquad (3\text{-}4)$$

$$CH_2 + CH_4 \rightarrow 2CH_3 \qquad (3\text{-}5)$$

$$2CH_3 \rightarrow C_2H_6 \qquad (3\text{-}6)$$

The activation energy is similar for both these reactions, with investigations reporting values ranging between 86 to 103 kcal/mole (14:54). Most likely, then, both reaction schemes take place during the decomposition of methane. Chou (6:279-281) has shown that methyl radicals exist in significant quantities during methane pyrolysis, while studies with deuterated methane (CD_4) indicate the presence of CH_2 (16:396-400).

Ethane to Ethylene

After its formation, ethane undergoes a series of dehydrogenation reactions, again probably involving the

methyl radical. The first dehydrogenation reaction forms ethylene from ethane. The most likely mechanism for the reaction is (5:4-5):

$$CH_3 + C_2H_6 \rightarrow CH_4 + C_2H_5 \qquad (3\text{-}7)$$

$$C_2H_5 \rightarrow C_2H_4 + H \qquad (3\text{-}8)$$

$$H + CH_4 \rightarrow CH_3 + H_2 \qquad (3\text{-}9)$$

Resulting in the net reaction:

$$C_2H_6 \rightarrow C_2H_4 + H_2 \qquad (3\text{-}10)$$

Ethylene to Acetylene

Ethylene is similarly dehydrogenated into acetylene by reactions with radical species (5:4-5):

$$CH_3 + C_2H_4 \rightarrow CH_4 + C_2H_3 \qquad (3\text{-}11)$$

$$C_2H_3 \rightarrow C_2H_2 + H \qquad (3\text{-}12)$$

$$H + CH_4 \rightarrow CH_3 + H_2 \qquad (3\text{-}9)$$

With the net reaction:

$$C_2H_4 \rightarrow C_2H_2 + H_2 \qquad (3\text{-}13)$$

Carbon Deposition from Acetylene

Finally, acetylene dehydrogenates into solid carbon (5:5-6):

$$CH_3 + C_2H_2 \rightarrow CH_4 + C_2H \qquad (3\text{-}14)$$

$$C_2H \rightarrow C_{2(s)} + H \qquad (3\text{-}15)$$

$$H + CH_4 \rightarrow CH_3 + H_2 \qquad (3\text{-}9)$$

Resulting in the net reaction:

$$C_2H_2 \rightarrow C_{2(s)} + H_2 \qquad (3\text{-}16)$$

The mechanism for this final stage of methane decomposition is subject to debate. At temperatures around 500-700 K, acetylene appears to adsorb to the reaction container surface, where it then reacts to release the hydrogen. At higher temperatures, the reaction seems to take place in the gas stream, where solid carbon particles are formed which then deposit on the surface (31:2731-2734).

Additionally, deposition rates vary with the type of surface material involved (17:69-80). Different surfaces provided a different number of sites available for a molecule to adsorb or attach. Beyond that, some surfaces may play an active role in carbon deposition.

Methane also undergoes several secondary reactions during its decomposition, leading to propylene (C_3H_6), propyne (CH_3CCH), and other higher order hydrocarbons (5:4-5). But although a large number of different species are produced in methane decomposition, the total percentage of methane that decomposes is quite small for temperatures below 1200 K. Experiments at this temperature to study methane decomposition in a flow situation have produced less than 3% total conversion of methane to other species (5:6-7). Therefore, the effect of these many product species on the overall composition of the propellant gas is nominal.

Reaction Kinetics

While methane decomposes through several intermediate stages, the kinetics of the process are near first order in nature. Kozlov and Knorre (15:253-263) compared the rate constants for the individual reactions involved in methane decomposition and found that for temperatures below 1800 K, the conversion of methane to ethane dominates the kinetics

of the reaction. This first conversion then controls the overall reaction process, and the overall rate constant is then near first order for the temperature range of resistojet operation. A first order kinetic equation can then be used to express the decomposition of methane. The equation will have the form:

$$r = k[CH_4] \qquad (3\text{-}17)$$

where r is the rate of conversion of methane to daughter products, k is the rate constant, and $[CH_4]$ is the molar concentration of methane.

The rate constant itself will be temperature dependent, and of the form:

$$k = A\exp(-E/RT) \qquad (3\text{-}18)$$

where A is a constant, E represents the activation energy of the reaction, and R is the gas constant.

This temperature dependent rate constant has been estimated experimentally in several investigations (15:253-263; 21:348-353; 22:709-711). A comparison of these rate constants is shown in Figure 3-1.

If the kinetic equation is modified to use the pressure of methane rather than molar concentration, the basic form

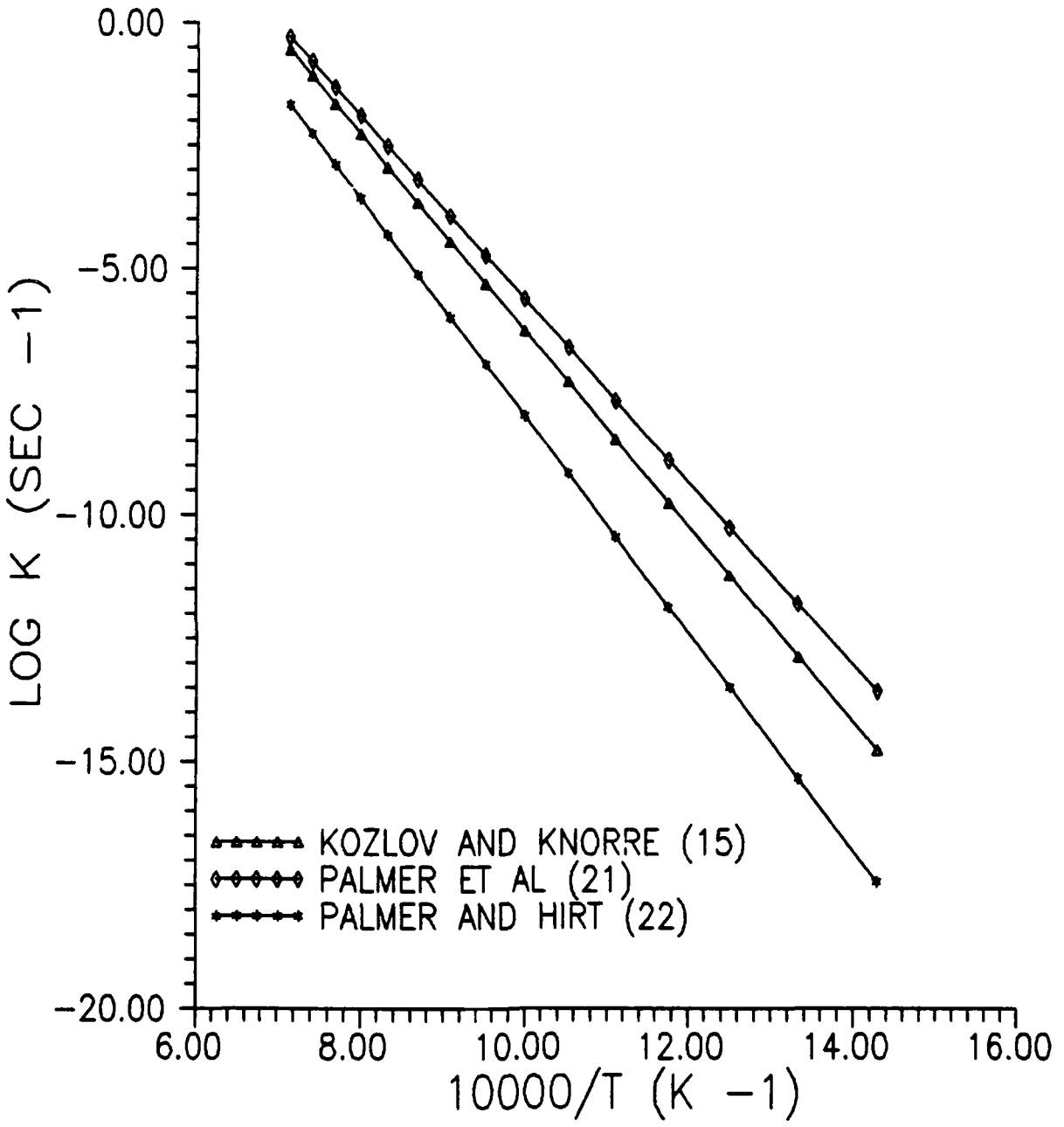

Figure 3-1. Rate Constant Estimates for the Decomposition of Methane

of the equation remains almost unchanged. Equations 3-17 and 3-18 can then be combined to give (8:39-50):

$$r=Aexp(-E/RT)P_{CH_4} \qquad (3\text{-}19)$$

where A = 25 mole/l sec atm, E=16200 cal/mole, and P_{CH_4} is the methane pressure. Equation 3-19 was experimentally obtained from methane up to 2000 K.

This investigation will use the pressure based Equation 3-19 because it offers several advantages. First, the equation was developed for pure methane as well as methane in mixture. Second, the equation was developed over a temperature range comparable to the operating conditions of the resistojet. Third, a rate equation which is a function of pressure is easily adaptable towards the study of resistojets.

IV. Heat Exchanger Analysis

By applying the principles of heat transfer and fluid mechanics, and using the results of studies done on laminar flow heat exchangers of unusually shaped channels, the performance of the space station resistojet can be analyzed. With this knowledge, the effects of carbon deposition on the resistojet can be determined.

This investigation analyzes the heat exchanger by splitting it into small sections, incrementally determining the heat transfer to the fluid section by section. The following assumptions were made for this approach:

1. Steady, fully developed laminar flow exists throughout the heat exchanger.

2. Heat exchanger channel surface temperatures are constant within a section.

3. Heat exchanger entrance conditions for the fluid are known.

4. The fluid behaves as a perfect gas.

5. No heat is transferred laterally within the fluid.

6. Fluid properties such as specific heat, viscosity, and thermal conductivity are constant within a section, but can vary between sections.

7. The resistojet heater maintains a constant heat flux.

8. Only a very small portion of methane decomposes in the heat exchanger, so that thermal energy losses due to chemical reactions may be neglected.

9. The pressure change due to fluid temperature change is small compared to the friction loss.

10. The gas enters the heat exchanger near room temperature (300 K).

These assumptions will be further developed below. A sketch of a channel section is shown in Figure 4-1.

For fully developed internal flow in the heat exchanger, the heat flux between the heater and the propellant fluid (q''_f) may be calculated from Newton's law of cooling (12:341):

$$q''_f = h(T_s - T_m) \qquad (4\text{-}1)$$

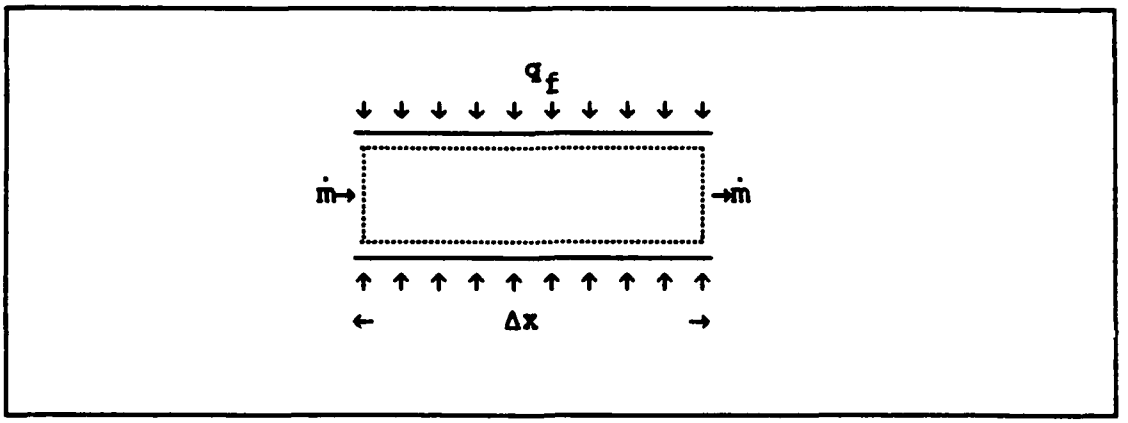

Figure 4-1. Mass and Energy Flow for a Channel Section

where h is the local convection heat transfer coefficient, T_s is the surface temperature of the heat exchanger, and T_m is the mean temperature of the fluid.

Heat transfer may also be measured with respect to the fluid passing through the heat exchanger. For a small section, the increase in fluid temperature will be small, and the gas specific heat at constant pressure (c_p) can be assumed as constant. The heat transfer to the fluid can then be expressed as (12:346-347):

$$q = \dot{m}c_p(\Delta T_m) \tag{4-2}$$

where $\dot{m}$ is the mass flow rate of the fluid, and ΔT_m represents the change in fluid temperature through the section of heat exchanger considered.

If the channel section length is small, its lateral increase in surface temperature will also be small, and may be assumed as constant. The heat transfer rate can then be considered constant across the area of heat transfer (A), which is the surface area of the channel section. Since the change in fluid temperatures will be small between sections, the lateral fluid heat flux will be small as well, and the heat transfer to the fluid may be found from the channel surface heat flux by:

$$q_f = q''_f A \tag{4-3}$$

Equation 4-1 may then be written as:

$$q_f = hA(T_s - T_m) \tag{4-4}$$

or, alternatively as:

$$q_f = \frac{(T_s - T_m)}{(1/hA)} \tag{4-5}$$

If a layer of carbon is deposited along the side of the tube, the deposit will effect the heat transfer rate based on the thermal conductivity of the carbon (k_c). The total heat transfer may then be expressed as (12:66):

$$q_f = \frac{(T_s - T_m)}{(1/hA) + (\delta/k_c A)} \qquad (4\text{-}6)$$

Equation 4-6 can be simplified as:

$$q_f = \frac{(T_s - T_m)Ahk_c}{(k_c + \delta h)} \qquad (4\text{-}7)$$

The total surface area of the channel section can be expressed as the cross-sectional perimeter of the exchanger channel (P) times the section length (Δx), or:

$$A = P\Delta x \qquad (4\text{-}8)$$

Substituting Equation 4-8 into Equation 4-7 gives the following expression for heat transfer in a small section:

$$q_f = \frac{(T_s - T_m)hk_c P\Delta x}{k_c + \delta h} \qquad (4\text{-}9)$$

If Equations 4-2 and 4-9 are combined, and the resulting expression is solved for ΔT_m, then the following equation is obtained describing the increase in fluid temperature through the heat exchanger channel section:

$$\Delta T_m = \frac{(T_s - T_m)hk_c P\Delta x}{\dot{m}c_p(k_c + \delta h)} \qquad (4\text{-}10)$$

For a small section of the heat exchanger ΔT_m will be very small, and the value of T_m as it enters the section can be used in the right side of Equation 4-10 to obtain a solution.

Once the fluid heat transfer coefficient is determined, equation 4-10 can be applied incrementally along the length of a heat exchanger channel to determine the total increase in fluid temperature as it passes through the exchanger.

Heat Transfer Coefficient (h)

The local heat transfer coefficient describes the heat flux between the heat exchanger and the fluid. The convection heat transfer process in a heat exchanger varies with the fluid properties and the fluid motion.

As the fluid enters a channel, the heat transfer coefficient is also highly dependent upon temperature. But once the flow in the exchanger becomes fully developed, the coefficient becomes independent of the temperature difference between the fluid and the channel wall. (28:86-87).

For forced convection, the heat transfer coefficient may be found from the fluid's Nusselt number (Nu), which relates the heat flux to the fluid properties, the fluid flow, and the channel geometry. For fully developed laminar

flow, the Nusselt number is constant (28:90), and is given by the equation (1:396-399):

$$Nu = hD/k_f \tag{4-11}$$

where D is the diameter of the channel, and k_f is the thermal conductivity of the fluid.

Solving for h, Equation 4-11 becomes:

$$h = Nuk_f/D \tag{4-12}$$

For the resistojet, the problem of determining h is complicated by the shape of the channel, as shown in Figure 4-2.

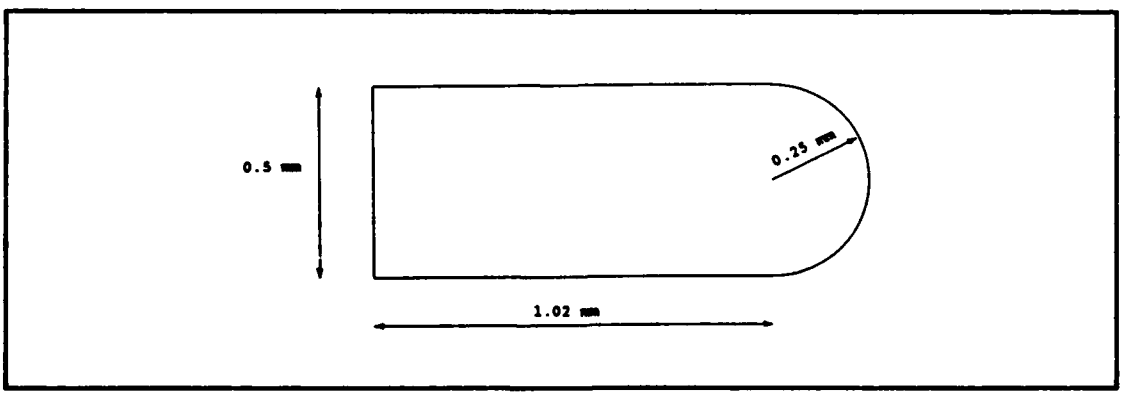

Figure 4-2. Resistojet Heat Exchanger Channel

The term for diameter in equation 4-12 must then be replaced by the hydraulic diameter for the channel, given by the equation (28:89-90):

$$D_h = 4A/P \qquad (4\text{-}13)$$

A value for the Nusselt number must then be determined for the channel shape and flow conditions. For turbulent flow, the Nusselt number in a non-circular channel will resemble that for a circular channel. The resistojet heat exchanger, however, will heat fluid in laminar flow, as defined by the Reynolds number for fluid flow (28:89-90):

$$Re = \dot{m}D_h/A\mu \qquad (4\text{-}14)$$

Re<2300 for laminar flow
Re>4000 for turbulent flow

where μ is the fluid viscosity. For the resistojet, the hydraulic diameter for the heat exchanger channel is 0.07316 cm and Reynolds number values for flow entering the heat exchanger are usually less than 500 (18:197-203).

In laminar flow, the Nusselt number becomes highly dependent on the channel shape and flow profile. Shah (28:75-108) has studied the laminar flow in non circular flow channels of various cross-sectional shapes, and has found that the Nusselt number remains constant for a given

channel geometry and heat flux boundary condition. Shah then developed a method for determining the Nusselt number for a wide variety of channel shapes and heat flux conditions.

By approximating the resistojet heat exchanger channel shape as a rectangle, and assuming a constant channel heat flux within each section, then the Shah results may be applied to the heat exchanger to determine the Nusselt number for propellant flow. For a channel length of 0.127 cm, and a channel width of 0.05 cm, the corresponding Nusselt number is 4.50 (28:96).

These results can be substituted into Equation 4-12 to obtain:

$$h = 4.50k_f/D_h \tag{4-15}$$

Reynolds number and hydraulic diameter can also be used to check that fully developed flow exists throughout the heat exchanger. When laminar fluid flow enters a channel, the length required to establish fully developed conditions (x_{fd}) can be approximated from the equation (12:334-335):

$$x_{fd} \approx 0.05ReD_h \tag{4-16}$$

For the resistojet hydraulic diameter and typical operating Reynolds number (<500), the required distance to

establish fully developed laminar flow in the heat exchanger is 1.83 cm. Since the propellant flow in the resistojets is separated into the individual channels 6 cm before entering the heat exchanger (19), the assumption of fully developed flow throughout the exchanger is valid.

Fluid Pressure

The studies by Shah also provide a means to determine the propellant pressure loss in the heat exchanger channel. This can be used to compute an adjusted value for gas pressure for any section in the heat exchanger, which can then be used in Equation 3-19 to determine the methane decomposition rate for that section.

For laminar flow, the pressure loss due to friction in a channel (dp/dx) may be found by the following equation (28:88-89):

$$\frac{dp}{dx} = \frac{-f\rho u_m^2}{D_h} \qquad (4\text{-}17)$$

where ρ is the fluid density, u_m is the fluid mean velocity, and f is the Fanning friction factor, which relates wall shear stress to flow kinetic energy.

For a small section of the heat exchanger channel of length Δx, the resulting pressure change can be represented by Δp, resulting in the equation:

$$\frac{\Delta p}{\Delta x} = \frac{-f\rho u_m^2}{D_h} \qquad (4\text{-}18)$$

The fluid mean velocity can be found by the equation:

$$u_m = \dot{m}/\rho A \qquad (4\text{-}19)$$

The fluid density can be found from the universal gas law:

$$\rho = p/RT_m \qquad (4\text{-}20)$$

If these substitutions are made into Equation 4-17, and the results solved for Δp, the resulting equation is:

$$\Delta p = \frac{f\Delta x\dot{m}^2 RT_m}{D_h A^2 p} \qquad (4\text{-}21)$$

Since the pressure change in a small section of the channel will itself be very small, the pressure of the fluid as it enters the section will not differ much from the exit

pressure, and this value can then be used in the right side of Equation 4-21.

The Fanning friction factor can be obtained from the flow conditions and channel geometry in the same manner as the Nusselt number. For laminar flow in a channel, the product of the Fanning friction factor and the flow Reynolds number is constant for a given channel cross-sectional shape (28:92-93):

$$fRe = \text{constant} \qquad (4\text{-}22)$$

By approximating the shape of the resistojet heat exchanger to the rectangle used to find the Nusselt number, and applying the results obtained by Shah, the value of the constant in Equation 4-22 becomes 16.43 (28:96-99). Equation 4-22 can then be rewritten for the resistojet as:

$$f = 16.43/Re \qquad (4\text{-}23)$$

The Fanning friction factor in the heat exchanger therefore becomes a function of the flow Reynolds number. This function can then be evaluated and used in Equation 4-21 to calculate the pressure loss due to friction through the heat exchanger.

The fluid pressure will also change due to the change in gas composition as methane decomposes, and from the

increase in gas temperature. However, since only a very small amount of methane is actually broken down in the heat exchanger, any corresponding pressure change will be negligible.

The pressure loss from the gas temperature change is also negligible when compared to friction losses. A typical operation of the resistojet will heat 0.35 Kg/hr of methane entering at 1.5 atm pressure and 300 K, to 1200 K. For an ideal gas obeying conservation of mass and momentum, the resulting pressure loss is 0.0006 atm. The friction loss under the same conditions is 0.013 atm (see Table 6-1). The pressure loss due to temperature is not significant next to the friction loss, and Equation 4-21 may be used to compute the overall pressure loss in the heat exchanger.

With Equation 4-21, the pressure along the length of the heat exchanger can be incrementally determined. If the exchanger is analyzed with methane as the propellant, these values for pressure can be used in Equation 3-19:

$$r = A\exp(-E/RT)P_{CH_4} \qquad (3\text{-}19)$$

to compute the local rate of methane decomposition in the heat exchanger channels as a function of the flow conditions.

Carbon Deposition

Equation 3-19 describes the rate of change in the molar concentration of methane (moles/l sec) in the heat exchanger channel. However, only a very small fraction of the radical species produced in the decomposition will ultimately deposit as carbon on the channel walls. This fraction may be found by the same technique used to determine fluid temperatures within the channel.

If a small sample of methane is considered passing through the section of channel of length Δx shown in Figure 4-1, the time that unit takes to pass through the section (Δt) can be found from the mean velocity of the fluid:

$$\Delta t = \Delta x / u_m \qquad (4\text{-}24)$$

This travel time can be multiplied by the product of Equation 3-19 to give the change in methane concentration within the section:

$$\Delta[CH_4] = r\Delta t \qquad (4\text{-}25)$$

The breakdown of one methane molecule produces one carbon atom in a form available for carbon deposition. Therefore, if the methyl radical is assumed to be the driving species of the overall deposition reaction, the

molar concentration of carbon atoms available for deposition can be represented by $[CH_3]$, and Equation 4-25 describes the increase in carbon radical formation.

If the value of $[CH_3]$ is assumed to be zero as the methane enters the heat exchanger, and Equations 3-19, 4-24, and 4-25 are applied incrementally along the length of the channel, the value for $[CH_3]$ at any section in the channel can be found.

Once the value for $[CH_3]$ is known, the flux of moles depositing on the channel walls (T) is given by (7):

$$T = \frac{\alpha[CH_3]\bar{c}}{4} \qquad (4\text{-}26)$$

where $\bar{c}$ is the mean molecular velocity of the radicals, the term $[CH_3]\bar{c}/4$ describes the molar flux of radicals colliding with the wall, and α is the molar fraction of particles which finally deposit on the channel wall, rather than bouncing off or forming a higher order hydrocarbon.

The velocity of a radical molecule within a sample of gas is a function of the kinetic energy of the molecule. The mean kinetic energy of all the particles in a gas sample is represented by the mean temperature of the sample. The mean molecular velocity (m/sec) for the radicals in the sample can be determined by the equation (7):

$$\bar{c} = \kappa(2\varepsilon/M)^{1/2} \qquad (4\text{-}27)$$

where ε is the mean kinetic energy of the molecules (eV), M is the molecular weight of the species (amu), and κ is equal to 1.389×10^{4}.

The fraction α describes several factors. For a radical molecule to deposit carbon on the channel wall, several conditions must be met. First, the molecule must undergo the conversions to acetylene, rather than forming some other hydrocarbon. Second, the molecule must find a site on the wall for the carbon to adsorb. Third, the molecule must undergo the final dehydrogenation reactions to produce the deposited carbon.

These factors depend upon the channel material and geometry, so that α can become unique for each application. However, with some simplifying assumptions, α can be estimated for the model resistojet.

Only a handful of studies have been made to study the deposition of carbon from methane specifically on platinum. One particularly useful study was performed by the Marquardt Company researching the development of a biowaste resistojet for NASA (23:30-45; 24:36-40). Carbon deposition rates were measured for methane under a variety of operating conditions similar to the operating conditions of the model resistojet.

The Marquardt Company passed methane at 2 atm in a steady flow through a 2 inch long, 0.037 inch inside

diameter tube heated to a constant temperature for up to 500 hours. This apparatus had a similar cross-sectional area to perimeter ratio (0.0235 cm) as the model resistojet heat exchanger channels (0.0183 cm). Test procedures were set up to simulate resistojet operating conditions. Test results showed a deposition rate steady with time, but increasing greatly along the tube in a downstream direction (23:31).

If the incremental process developed for the heat exchanger is applied to the Marquardt tests, a value for α can be obtained for those tests. Although the experimental tube geometry and operation differ somewhat from the model resistojet conditions, the situations are similar enough to use the value for α calculated from the Marquardt results and use it as an estimated α value for the model resistojet heat exchanger channel. By assuming that the deposition is uniform around the perimeter of the heat exchanger channel, the geometry of the channel section and the properties of carbon can be used to convert the flux value into a deposition rate (r_d) by the equation:

$$r_d = TP\Delta x M_c/\rho_c \qquad (4\text{-}28)$$

where M_c is the molecular weight and ρ_c the density of carbon.

For the Marquardt data, the average value of α obtained is 6.758×10^{-8}, which indicates that the fraction of

molecules that deposits is small compared to the radical concentration.

Carbon deposition in the heat exchanger is therefore computed in two first order steps. The first calculates the decomposition of methane into radical products by Equation 3-19. The second computes the carbon deposition rate from the radical concentration by Equation 4-28.

With the deposition rates known, the deposition thickness over time can be calculated and used to determine new channel dimensions and corresponding flow conditions. The two step deposition process can be applied for each channel section from the section flow conditions to determine a local deposition rate. Multiplying this rate by a unit of operating time gives a deposition thickness in the channel. The incremental process outlined in this chapter can then be repeated for the next time increment to calculate new flow conditions in each section, and thus a new carbon deposit thickness to be added to the previous one. This procedure can be repeated over a desired length of time to show the growth of the carbon deposit in the channel, and any corresponding changes in flow conditions.

V. Computer Program Development

From the equations derived in Chapter IV, a computer program was developed to simulate the operation of the experimental resistojet built by the Lewis Research Center (LRC). The program takes a set of heat exchanger inlet conditions, divides the heat exchanger into a number of small sections as developed in Chapter IV, and incrementally analyzes each section to determine outlet conditions. The program was developed for both methane and carbon dioxide propellants to take advantage of the experimental data obtained by LRC on the model resistojet with carbon dioxide as the propellant.

Program Set-up

The program starts with the input of the operating conditions to be simulated, including propellant mass flow rate, inlet pressure, power level, and total run time of resistojet operation. From this data, the surface temperature profile for the heat exchanger must be determined.

The channel surface temperature can be determined in conjunction with the fluid heat transfer analysis by performing an energy balance around each channel section, shown in Figure 5-1.

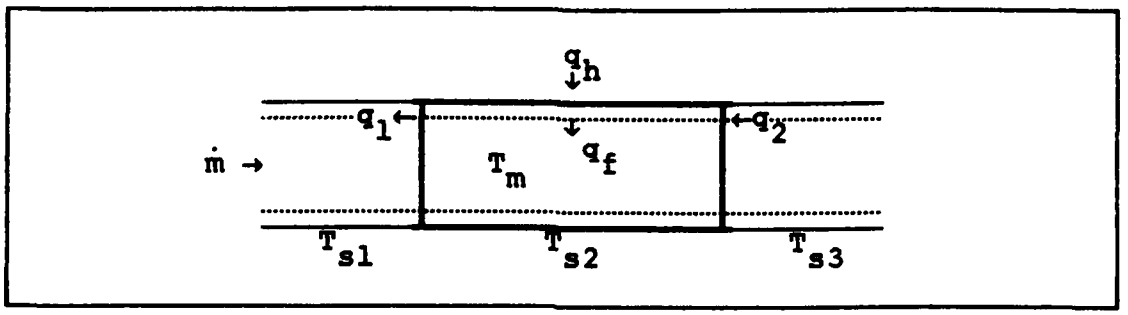

Figure 5-1. Energy Balance for a Channel Section

For a section of the channel wall at temperature T_{s2}, heat transfer occurs in four directions. First, heat is transferred from the resistojet heater to the channel wall (q_h). Second, heat is similarly passed laterally to the preceding section (q_1), which is at a slightly lower temperature (T_{s1}). Third, heat passes laterally along the channel wall from the succeeding section (q_2), which is at a slightly higher temperature (T_{s3}). Finally, heat is transferred from the channel wall to the fluid (q_f).

The energy balance for the channel section then becomes:

$$q_h + q_2 - q_1 - q_f = 0 \qquad (5\text{-}1)$$

Two additional assumptions are needed to solve this energy balance:

1. A constant heat flux is maintained from the resistojet heater, so that q_h is a constant for each heat exchanger section.

2. The heat exchanger entrance and exit are well insulated, so that q_1 for the first section and q_2 for the last section are approximately zero.

A constant q_h will be based on the resistojet power level (W). For a small section of the heat exchanger, the heat transfer from the corresponding small section of heater can be found by:

$$q_h = \frac{W\Lambda}{36S_n} \tag{5-2}$$

where S_n is the total number of heater sections, 36 represents the 36 channels of the heat exchanger, and Λ is a scaling factor which determines the fraction of heater power that is ultimately transferred to the heat exchanger.

If the surface temperatures of both the current and the preceding channel sections are known, then q_1 can be found by the equation (12:3-6):

$$q_1 = \frac{k_{pt}A_{pt}(T_{s1} - T_{s2})}{\Delta x} \tag{5-3}$$

where k_{pt} is the thermal conductivity of platinum, A_{pt} is the effective cross-sectional area of the platinum channel wall.

The value of q_f is given by Equation 4-9:

$$q_f = \frac{(T_s - T_m)hk_c P\Delta x}{k_c + \delta h} \qquad (4\text{-}9)$$

The values for q_h, q_1, and q_f can be placed into Equation 5-1 to solve for q_2. Equation 5-3 can then be rewritten for q_2 and solved to determine the surface temperature of the succeeding section:

$$T_{s3} = T_{s2} + \frac{\Delta x q_2}{k_{pt} A_{pt}} \qquad (5\text{-}4)$$

When the next section is analyzed, the present q_2 becomes the new q_1. The process is then repeated throughout the length of the heat exchanger.

For this procedure to be applied from the heat exchanger inlet to its exit, the surface temperature at the exchanger inlet (T_{s2} for the first section) must still be determined. By applying the assumption of a very small lateral heat loss from the heat exchanger exit, the entrance temperature can be solved by an iterative process.

The program makes an initial guess for the channel surface temperature in the first section of the heat

exchanger. With q_1 for the first section assumed to be zero and the fluid temperature to be 300 K, the program then solves the conditions for the subsequent sections until the exchanger outlet is reached. A value for q_2 for the last section is thus calculated. If the final q_2 value is not near zero, then the data generated by this run is discarded, the program corrects its initial inlet temperature guess, and the next iteration is performed. Once a final value for q_2 near zero is obtained, the program accepts the iteration and the data generated.

Physical Property Data

Data for the specific heats, viscosities, and thermal conductivities for the heat exchanger materials and propellants were obtained from several sources (11:279-420; 12:667-685; 20; 27:2-91 - 2-92; 30:86-87; 33:577-794). Multiple sources were required mainly because of the lack of consensus on the properties of methane at higher temperatures, especially thermal conductivity. The physical property values used will have an effect on the results of the program, and may limit its accuracy.

For the program, values for the thermal conductivity of methane below 600 K were obtained from Reference 33, which were in close agreement with several other studies. Thermal

conductivity values above 600 K were taken from Reference 30.

The program reads in, from separate data files, specific heat, viscosity, and thermal conductivity data for both carbon dioxide and methane, and thermal conductivity data for carbon and platinum, for a range of temperatures covering the operation of the resistojet. This creates a set of physical data tables within the program. A subroutine was created to interpolate the data from these tables when required.

When the program needs a value for a property, it calls the subroutine with the specified temperature and the property desired. The subroutine locates the table values above and below the specified temperature, then linearly interpolates the property value. The interpolated value is then returned to the program. This process is repeated for specific heat, viscosity, and thermal conductivity at each section, so that changes in these temperature dependant properties between sections are accounted for.

Program Testing

The program employs two empirical constants in its analysis of the heat exchanger: The power scaling factor (Λ), and the effective platinum channel wall cross-sectional surface area (A_{pt}). These constants were evaluated with the

experimental data accumulated on the engineering model resistojet by LRC (18:197-203). One test by LRC with a carbon dioxide propellant installed thermocouples at various points in the resistojet, including the heat exchanger inlet and outlet, to help develop a thermal map of the resistojet.

Operating conditions for this test were as follows:

1. Inlet pressure: 2.72 atm.

2. Operating power: 405 W.

3. Mass flow rate: 1.06 Kg/hr CO_2 total.

The measured heat exchanger inlet surface temperature for this run was 903 K, and the exit surface temperature was 1152 K.

These operating conditions were duplicated in the computer program, and the values of Λ and A_{pt} were adjusted until the desired channel surface temperature values were obtained. The resulting values for the program constants were 0.663 for Λ, and 4.97×10^{-3} m^2 for A_{pt}. The actual cross-sectional area of the platinum heater and heat exchanger is approximately $8.7 \times 10^{-4} m^2$ (19). This difference may be partially due to some lateral heat transfer occurring in the fluid, heater insulation, and heat exchanger core.

The values for Λ and A_{pt} can be placed into the program and run with the data from other resistojet tests, and the program results compared with the experimental results. The results of this comparison for both methane and carbon dioxide propellants, with heat exchanger outlet (nozzle chamber) temperatures computed by the program, are shown in Table 5-1.

The channel surface and fluid mean temperature profiles for the heat exchanger generated by the program are shown in Figure 5-2. At the entrance to the heat exchanger, a large temperature gradient exists between the fluid and the platinum surface, creating a sharp lateral rise in fluid temperature. About 2.5 cm from the heat exchanger entrance, the fluid mean temperature approaches the surface temperature, and both temperatures rise steadily towards the exchanger outlet.

The large temperature gradient in the entrance region will have an effect on methane decomposition and carbon deposition there. Gas flowing near the channel edge will be at a much higher temperature than the gas at the center, creating a wide variation in radical generation and concentration in the radial direction. The deposition model developed in this investigation will generate an average radical concentration for a point on the channel based on the fluid mean temperature, but near the heat exchanger entrance, these radical species will be concentrated near

Table 5-1. Comparison of Program and Experimental Results (18:201)

Gas	Mass Flow Rate (kg/hr)	Est. Chamber Temp. (K)	Predicted Specific Impulse (sec)	Measured Specific Impulse (sec)
CO_2	0.536	1290	130.5	110
	1.37	669	94.0	92.7
	1.06	1124	121.9	119
CH_4	0.374	798	159.0	162
	0.986	476	123.0	131
	0.312	1186	193.8	192
	0.839	650	143.5	155

Note: Predicted specific impulse calculated by Equation 6-10

the channel surface. The radicals may then have a greater opportunity to react with the wall and deposit than the model would indicate. Therefore, the deposition model may not be valid near the heat exchanger entrance.

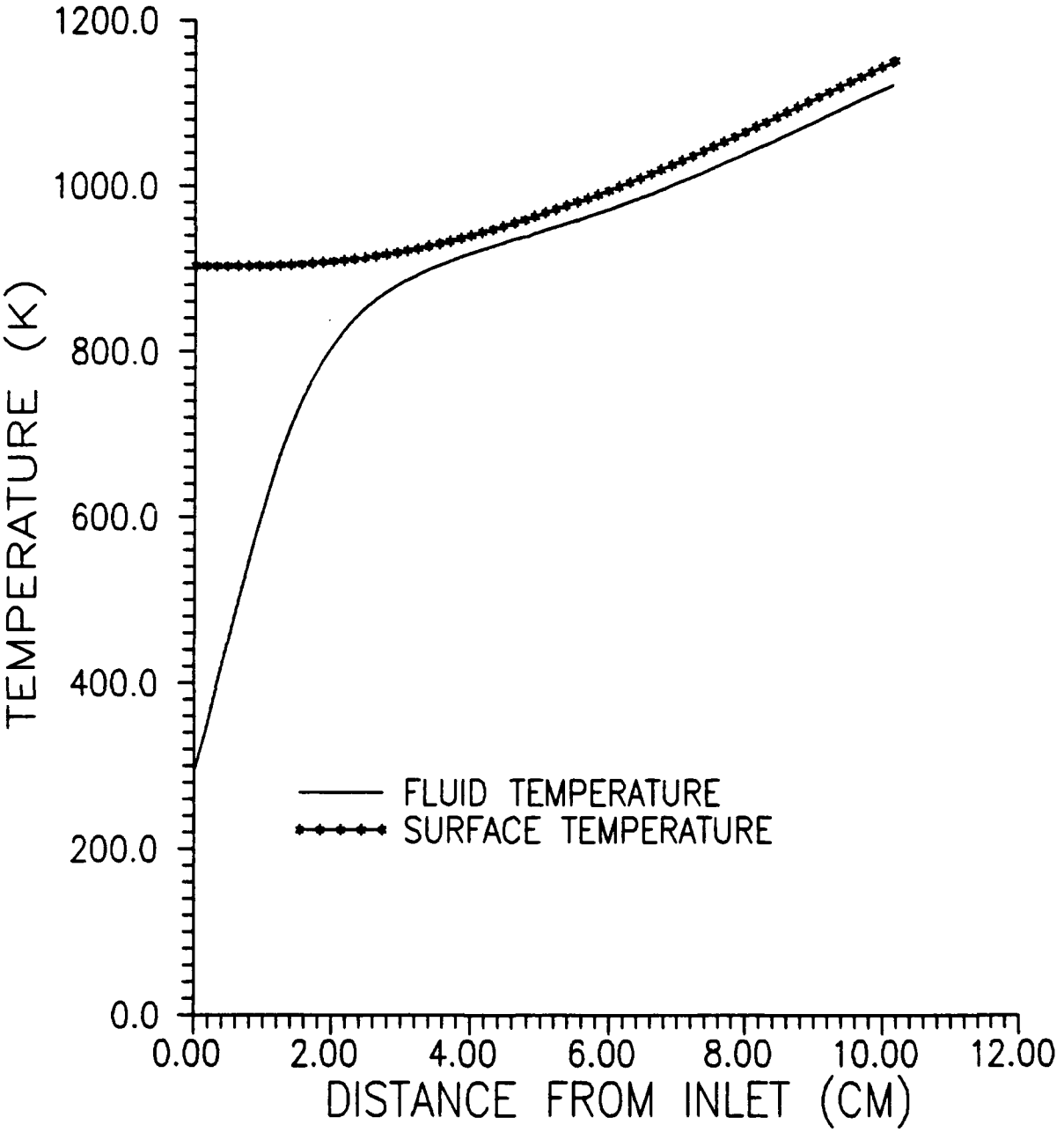

p = 2.7 atm **W = 405 W** **$\dot{m}$ = 1.06 Kg/hr CO_2**

Figure 5-2. Heat Exchanger Temperature Profile

Once the fluid mean temperature approaches the channel surface temperature, radical generation and concentration throughout a channel section will be more uniform, and carbon deposition should proceed as developed in the program.

While the available experimental data from the model resistojet is too limited to draw a final conclusion on the program's accuracy, the data does indicate a consistent analysis by the program of the resistojet's performance for heat exchanger outlet temperatures of 800-1200 K, which is the temperature range of this investigation.

The program was then tested by altering the allowable lateral heat loss from the ends of the heat exchanger, and altering the size of the heat exchanger channel axial sections. The addition of lateral heat losses from the exchanger had very little impact on the surface temperature profile obtained by the computer for heat loss values less than the value for heat transferred to the fluid in the first section. Altering the section size did alter the temperature profiles within the heat exchanger generated by the program, but did not alter the predicted channel outlet fluid temperature.

The results of this test are shown in Figure 5-3. The test compared the fluid temperature profile for a carbon dioxide propellant at a 1.06 Kg/hr flow rate at 405 W of operating power. The number of channel divisions made by

the program varied from 100 to 1000 in steps of 100 between program runs. As the number of channel divisions increased, the resulting change in the fluid temperature profile decreased, indicating a convergence in the analysis. For methane propellant simulation, the heat exchanger was divided into 1000 sections, resulting in a section length of about 0.1 mm.

With the tests completed, the heat exchanger analysis program was then used to simulate the operation of the engineering model resistojet with a methane propellant for a variety of operating conditions. A copy of the program is shown in Appendix C.

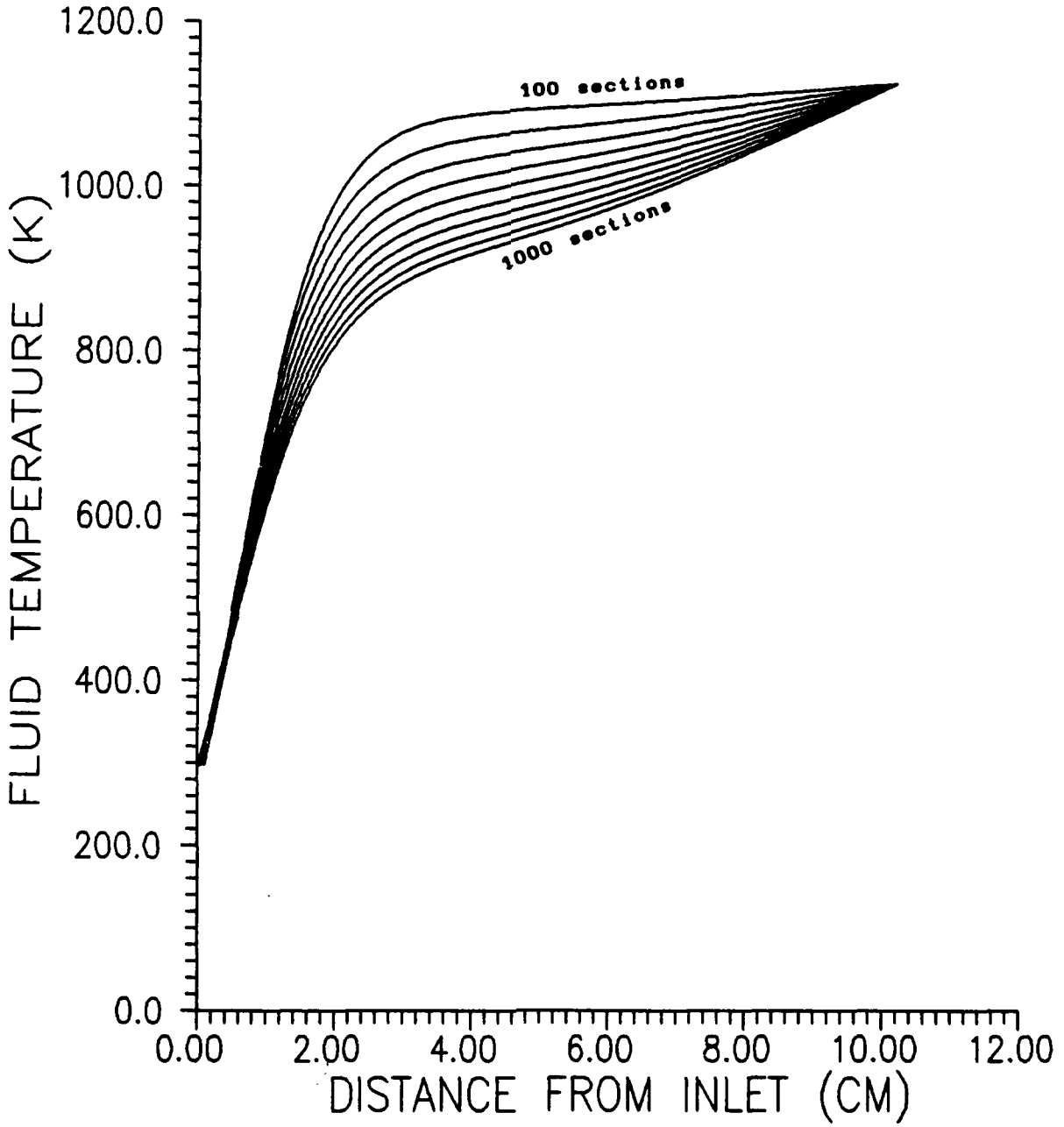

Figure 5-3. Fluid Temperature Profiles for Tests of Different Section Sizes

VI. Results and Discussion

The heat exchanger analysis program was run with a methane propellant to show the variation in exchanger performance and channel carbon deposition versus time, pressure, operating power, and mass flow rate. The heat exchanger channel section size used by the program was approximately 0.1 mm, and deposition was computed in one hour operating time intervals.

The key parameter in measuring performance is the propellant fluid temperature at the exchanger outlet. Higher fluid temperatures in the resistojet chamber will translate into higher nozzle exit velocities and propellant specific impulses (I_s), defined by the equation:

$$I_s = V_e/g_o \qquad (6\text{-}1)$$

where V_e is the exit velocity and g_o is the gravitational constant.

The results of the program analysis are presented below, and they show a wide variation in carbon deposition rates dependent upon the operating conditions of the resistojet.

Effect of Time

To measure the performance of the resistojet over time, a set of operating conditions had to be selected as a basis for analysis. These conditions should include fluid temperatures high enough to produce a significant amount of carbon deposition from methane, and be comparable to the experimental tests performed on the engineering model resistojet by NASA's Lewis Research Center (LRC).

The initial operating conditions chosen for the program were:

1. Inlet pressure: 1.5 atm.

2. Operating power: 500 W.

3. Mass flow rate: 0.35 kg/hr total.

These operating conditions produced a heat exchanger channel inlet surface temperature of 919 K, a channel outlet surface temperature of 1231 K, and an outlet fluid temperature of 1218 K.

The heat exchanger was then analyzed by the program for a period of 2000 hours, producing a carbon deposition thickness at the channel outlet of 98.55 μm, without any significant change in exchanger performance. The fluid exit

temperature remained unchanged, although several flow properties had changed due to deposition. The results of this analysis are shown in Table 6-1.

Table 6-1. Heat Exchanger Performance Over Time

Time of Operation (hours)	Outlet Fluid Temperature (K)	Outlet Surface Deposition (μm)	Fluid Pressure Loss (atm)	Outlet Reynolds Number
1	1218	0.06	0.013	101.5
50	1218	2.79	0.013	102.1
100	1218	5.62	0.013	102.7
500	1218	27.50	0.015	107.8
1000	1218	52.98	0.017	114.5
1500	1218	76.64	0.020	120.0
2000	1218	98.55	0.024	128.7

Inlet p = 1.5 atm W = 500 W $\dot{m}$ = 0.35 kg/hr

The profile of carbon deposition along the heat exchanger channel after 100 hours is shown in Figure 6-1. This profile is similar to the channel profiles for the rate of radical species generation (Figure 6-2), radical concentration (Figure 6-3), and carbon deposition rate (Figure 6-4). All these profiles retain their same basic shapes throughout operation. The extremely small value for the fraction of depositing molecules (α) means that the number of radicals that deposit on the channel wall is very small compared to the total number of radicals in a channel section, and so the radical concentration does not show a depreciation from deposition.

The fluid temperature profile remained unchanged throughout 2000 hours of operation, and is shown in Figure 6-5.

Flow properties, however, do show a change with time. As the hydraulic radius of the channel slowly decreases from carbon deposition, the fluid velocity must increase slightly to maintain the mass flow rate. Correspondingly, the fluid Reynolds number increases over time at any point in the channel, as shown in Figure 6-6. The changing flow conditions result in a small increase in the pressure loss in the channel, but even after 2000 hours of operation, the outlet pressure is still 99.3 % of its initial value.

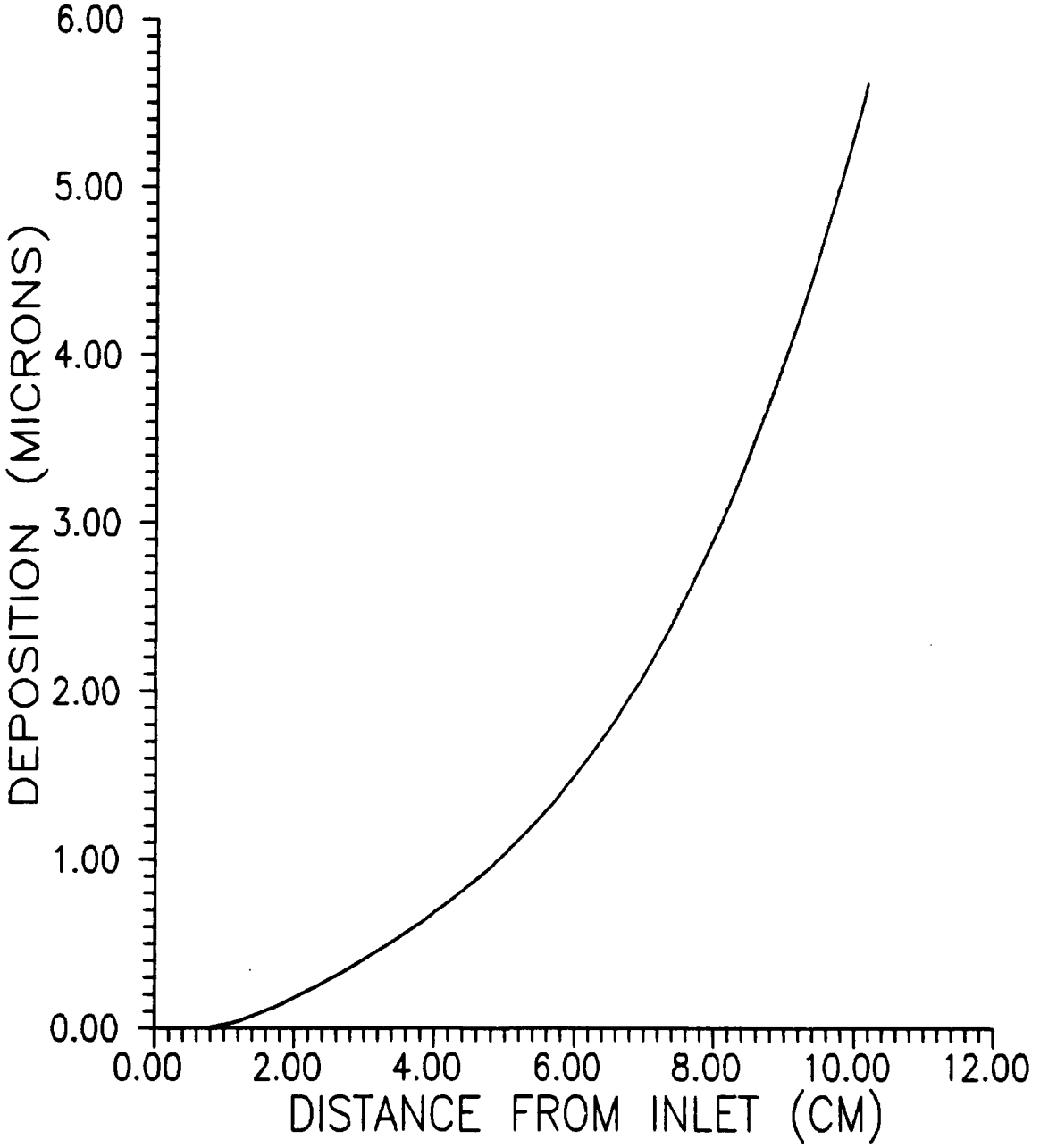

W = 500 W $\dot{m}$ = 0.35 kg/hr

Figure 6-1. Carbon Deposition Profile After 100 Hours at 1.5 atm

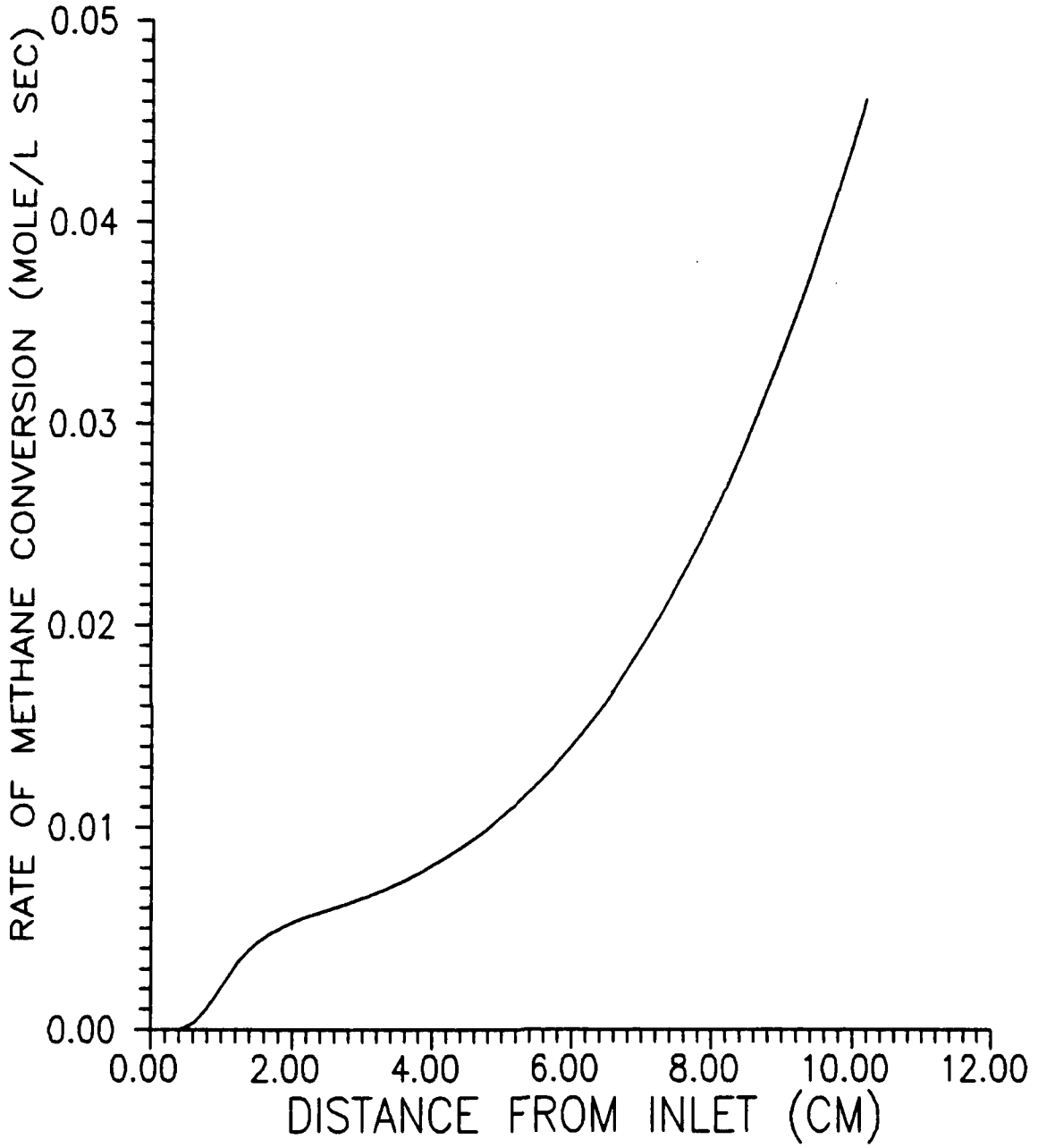

p = 1.5 atm W = 500 W $\dot{m}$ = 0.35 Kg/hr t = 100 hr

Figure 6-2. Methane Decomposition Profile

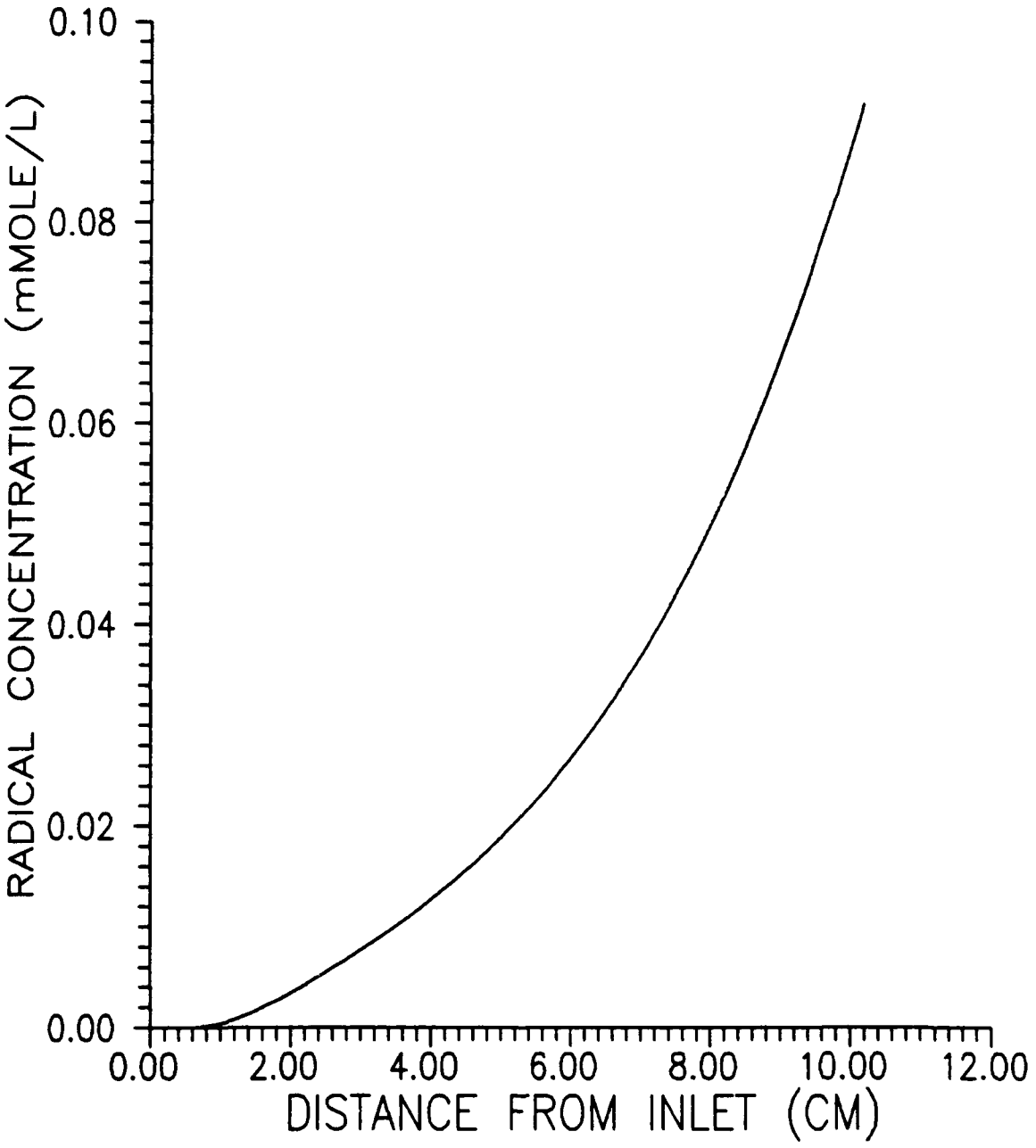

p = 1.5 atm W = 500 W $\dot{m}$ = 0.35 Kg/hr t = 100 hr

Figure 6-3. Radical Concentration Profile

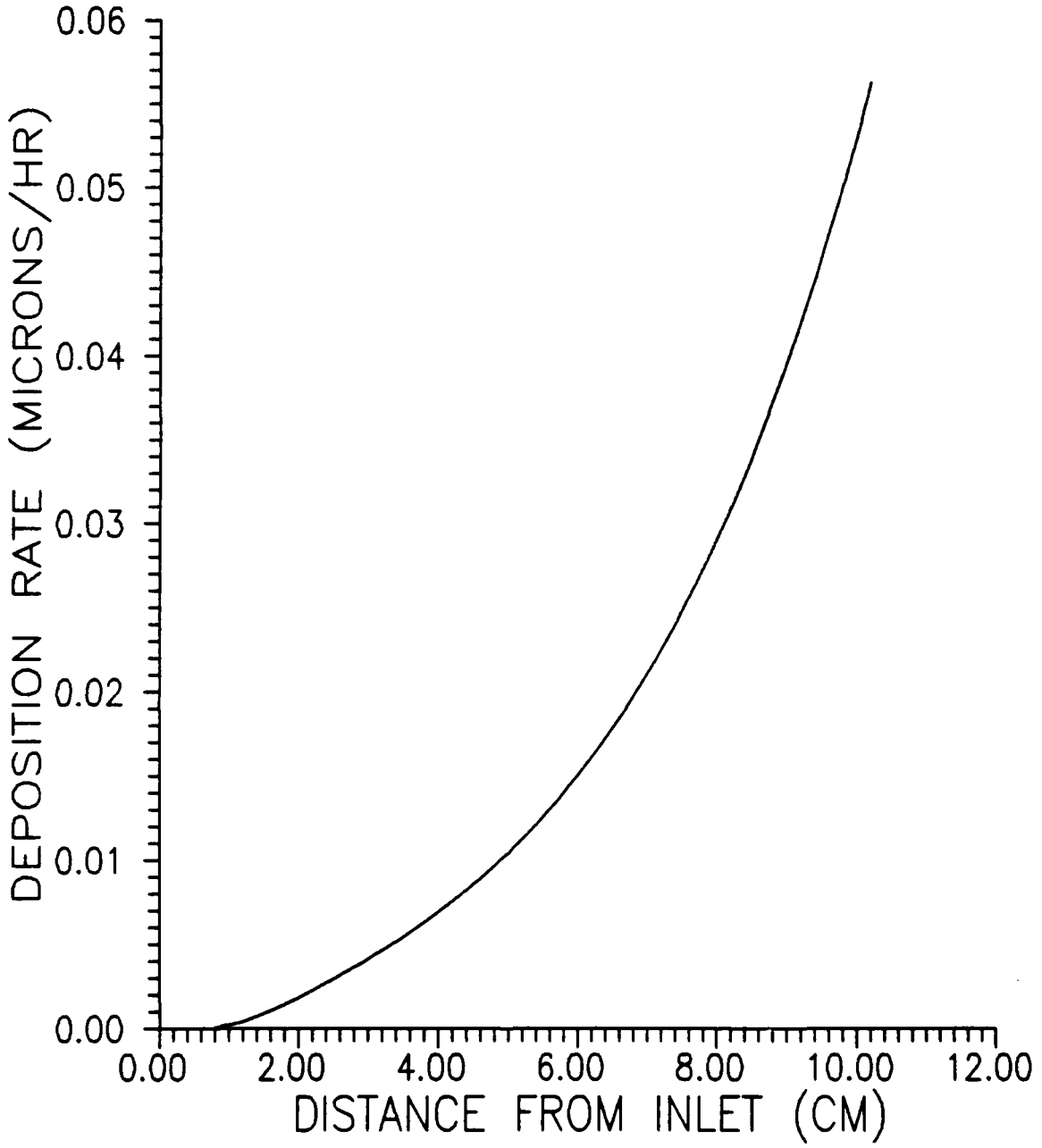

p = 1.5 atm W = 500 W $\dot{m}$ = 0.35 Kg/hr t = 100 hr

Figure 6-4. Carbon Deposition Rate Profile

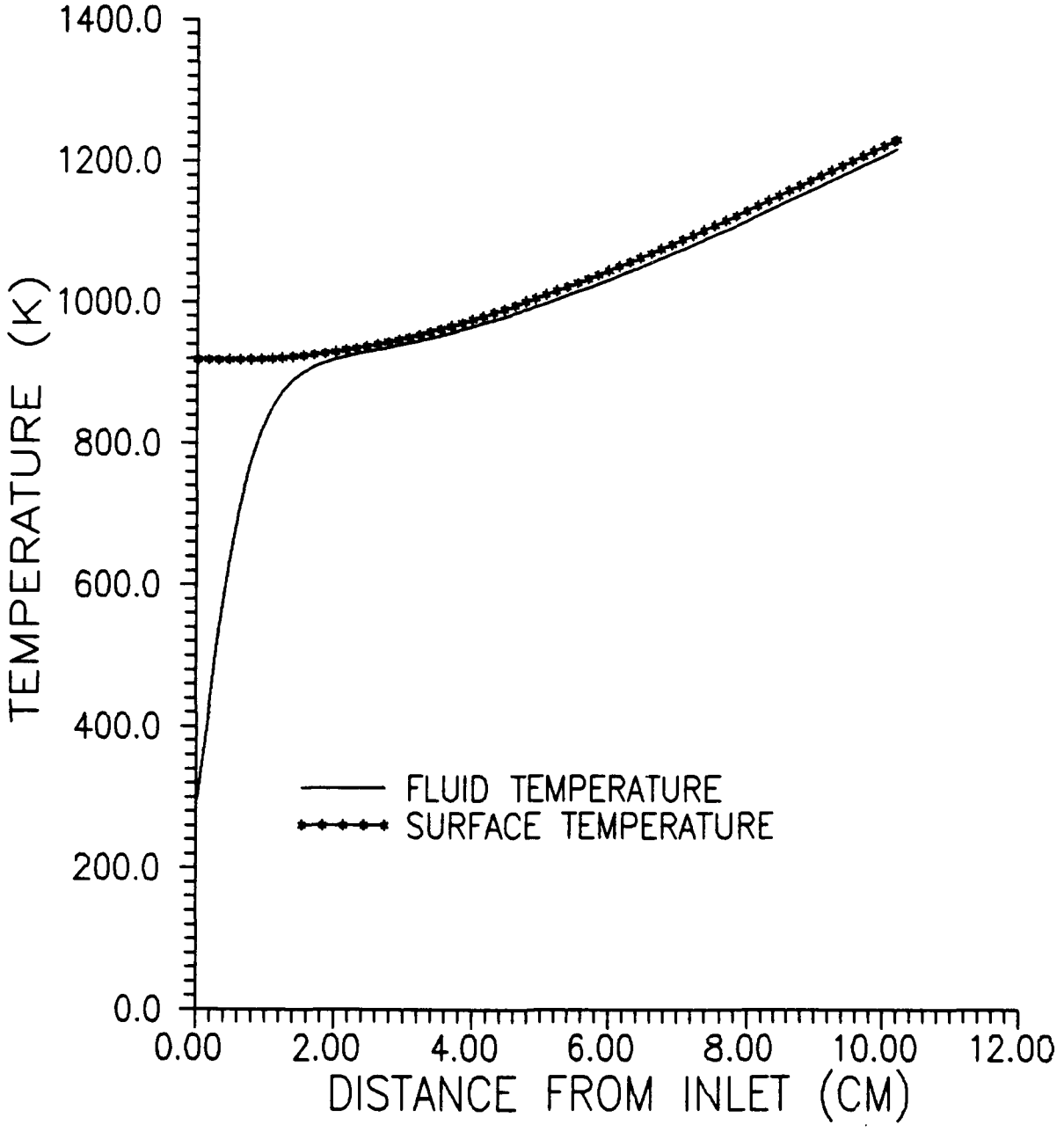

p = 1.5 atm W = 500 W $\dot{m}$ = 0.35 kg/hr

Figure 6-5. Heat Exchanger Temperature Profile

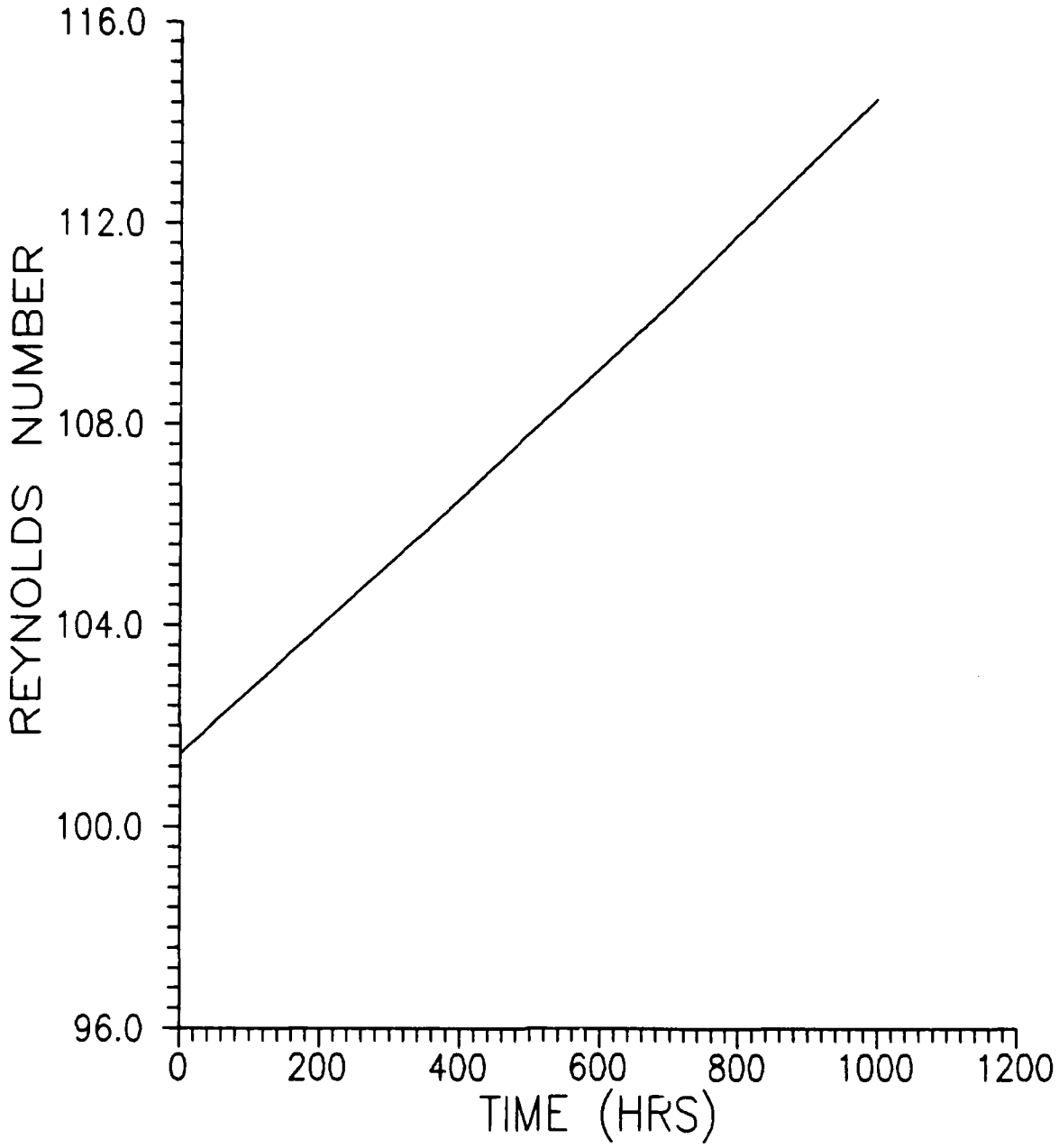

p = 1.5 atm W = 500 W $\dot{m}$ = 0.35 kg/hr

Figure 6-6. Cutlet Reynolds Number vs. Operational Time

The carbon deposition rate itself is affected by the shrinking hydraulic radius. As fluid velocity increases in the channel, the residence time of methane in the heat exchanger decreases, the number of methyl radicals produced also decreases, slowly reducing the carbon deposition rate. This decrease is reflected in Figure 6-7, which shows the channel outlet deposition thickness over time.

Additional data for the steady operation of the resistojet with methane at 1.5 atm is shown in Appendix A.

One factor which must be considered when analyzing carbon deposition is the uncertainty of the deposition process for carbon thicknesses over 20 μm. As platinum surface sites are covered by carbon, the depositing radicals will have fewer places to attach, and the nature of the deposition will change from carbon onto platinum, to carbon onto carbon. For experimental studies of carbon deposition from methane on prototype resistojets, carbon deposits above 19.5 μm have not been studied (23:30-45). The loss of surface sites may also lead to the significant formation of solid carbon in the gas stream, which could impact the overall performance of the resistojet.

Even with these uncertainties, though, the program does indicate that a significant amount of carbon could be deposited on the heat exchanger channel walls without impacting the heat transfer.

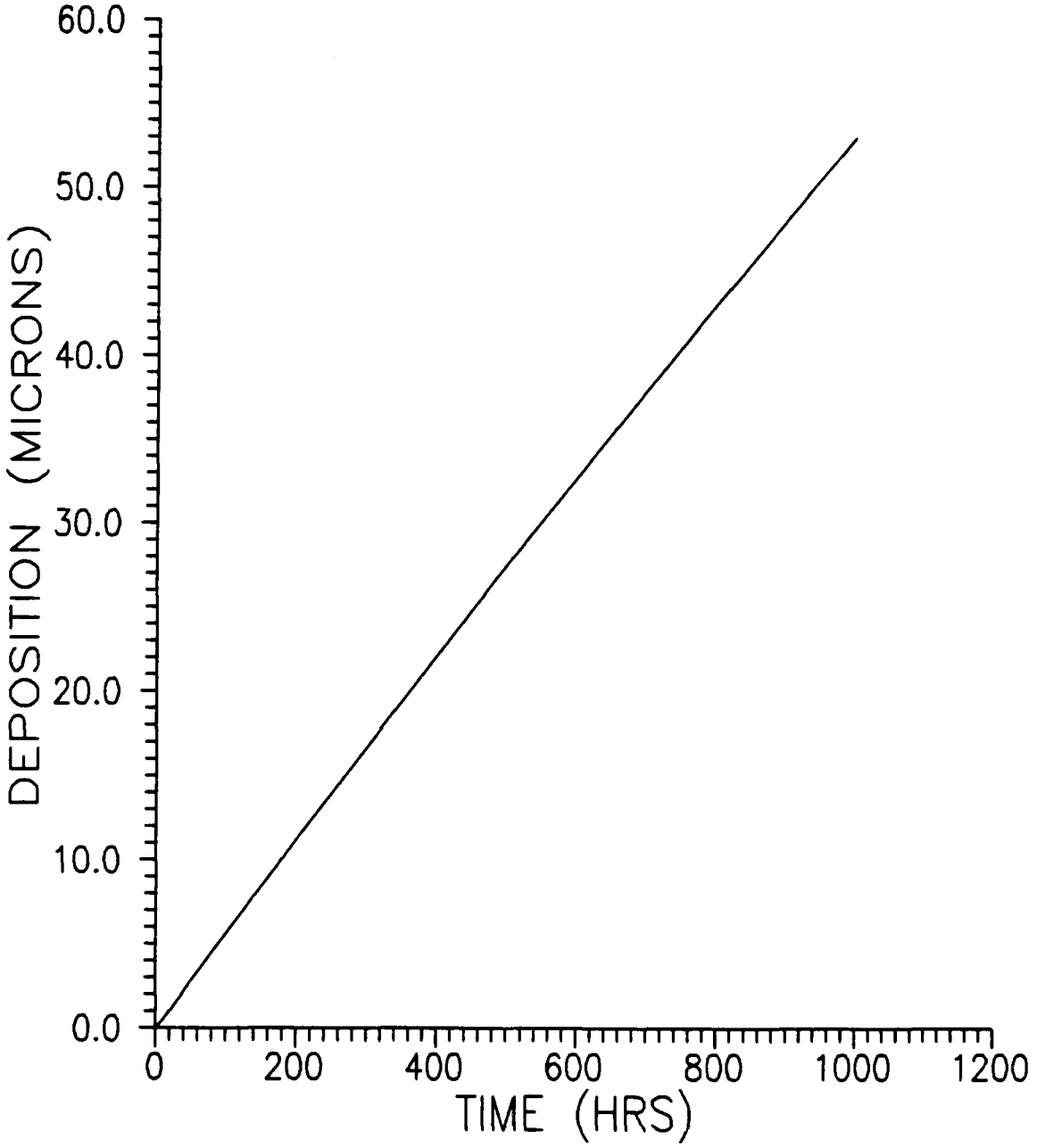

p = 1.5 atm W = 500 W $\dot{m}$ = 0.35 kg/hr

Figure 6-7. Channel Outlet Deposition vs. Operational Time

Effect of Pressure

The carbon deposition rate is directly related to methane pressure. This dependence is illustrated by the program when the surface deposition is measured for the exchanger channel exit at various pressures. Figure 6-8 shows an increase in carbon deposition as the operating pressure is increased.

The effect of pressure can also be shown by repeating the initial exchanger analysis performed above with a higher operating pressure. Doubling the pressure created roughly a four-fold increase in the deposition rate. The 100 hour surface deposition profile for 3 atm operation is shown in Figure 6-9, and can be compared to the profile for 1.5 atm shown in Figure 6-1. Additional data on 3 atm operation is shown in Appendix B.

The results of varying pressure in this investigation indicate that the carbon deposition rate can be greatly affected by operating pressure, and that deposition in the resistojet from methane at high temperatures can be reduced by running the resistojet at lower pressures. Lower pressures, though, force a trade off resulting in a lower thrust.

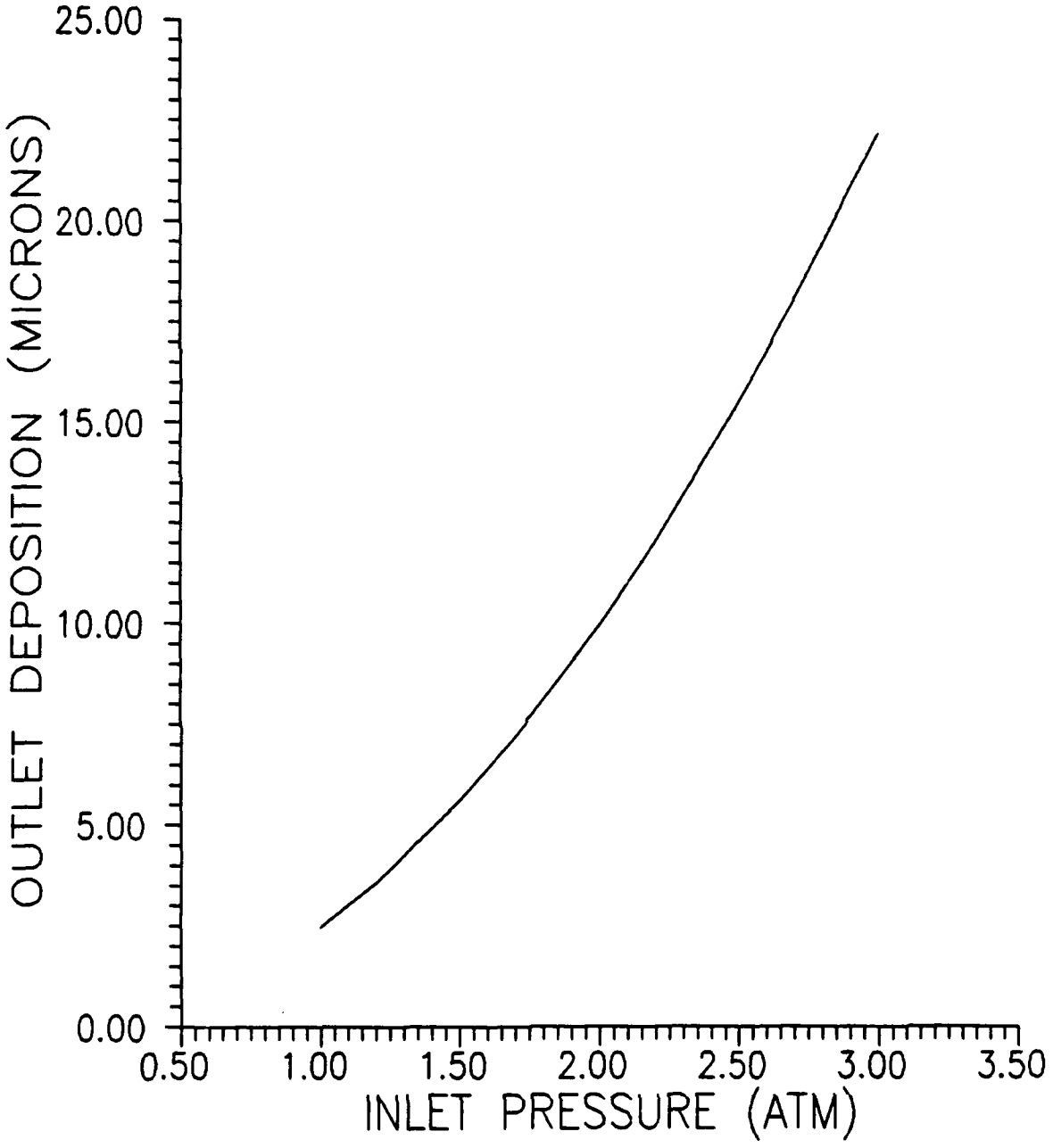

W = 500 W $\dot{m}$ = 0.35 kg/hr t = 100 hours

Figure 6-8. Carbon Deposition vs. Operating Pressure

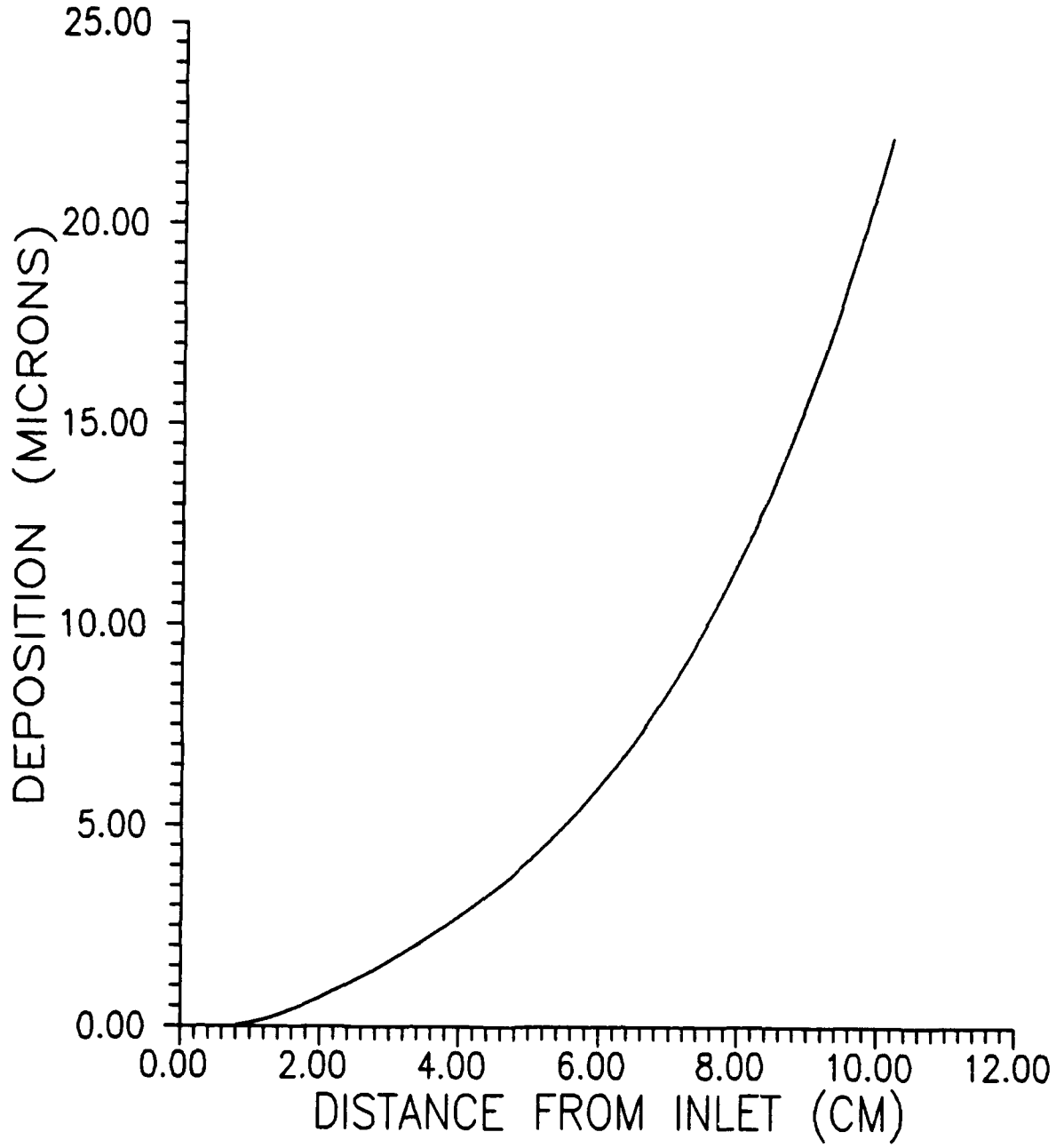

W = 500 W **$\dot{m}$ = 0.35 kg/hr**

Figure 6-9. Carbon Deposition Profile After 100 Hours at 3 atm

Effect of Operating Power

The operating power of the resistojet will ultimately determine the temperature profile along the heat exchanger channel, and so determine the carbon deposition rate in the exchanger.

For a constant pressure and mass flow rate, the propellant temperature is almost linearly related to the resistojet power level, as shown in Figure 6-10. The fluid temperature in turn drives the carbon deposition rate inside the channel, and this relationship is illustrated by Figure 6-11. Carbon deposition increases significantly as the fluid temperature rises above 900 K, which conforms to experimental observations (23:30-45).

The net effect of power on carbon deposition, shown in Figure 6-12, reflects the impact of fluid temperature on deposition, and indicates how greatly the deposition rate will increase for even small increases in power.

Effect of Mass Flow Rate

Thrust for the resistojet will primarily be the product of the resistojet total mass flow rate and the propellant exit velocity (25), or:

$$F \cong \dot{m} V_e \qquad (6\text{-}2)$$

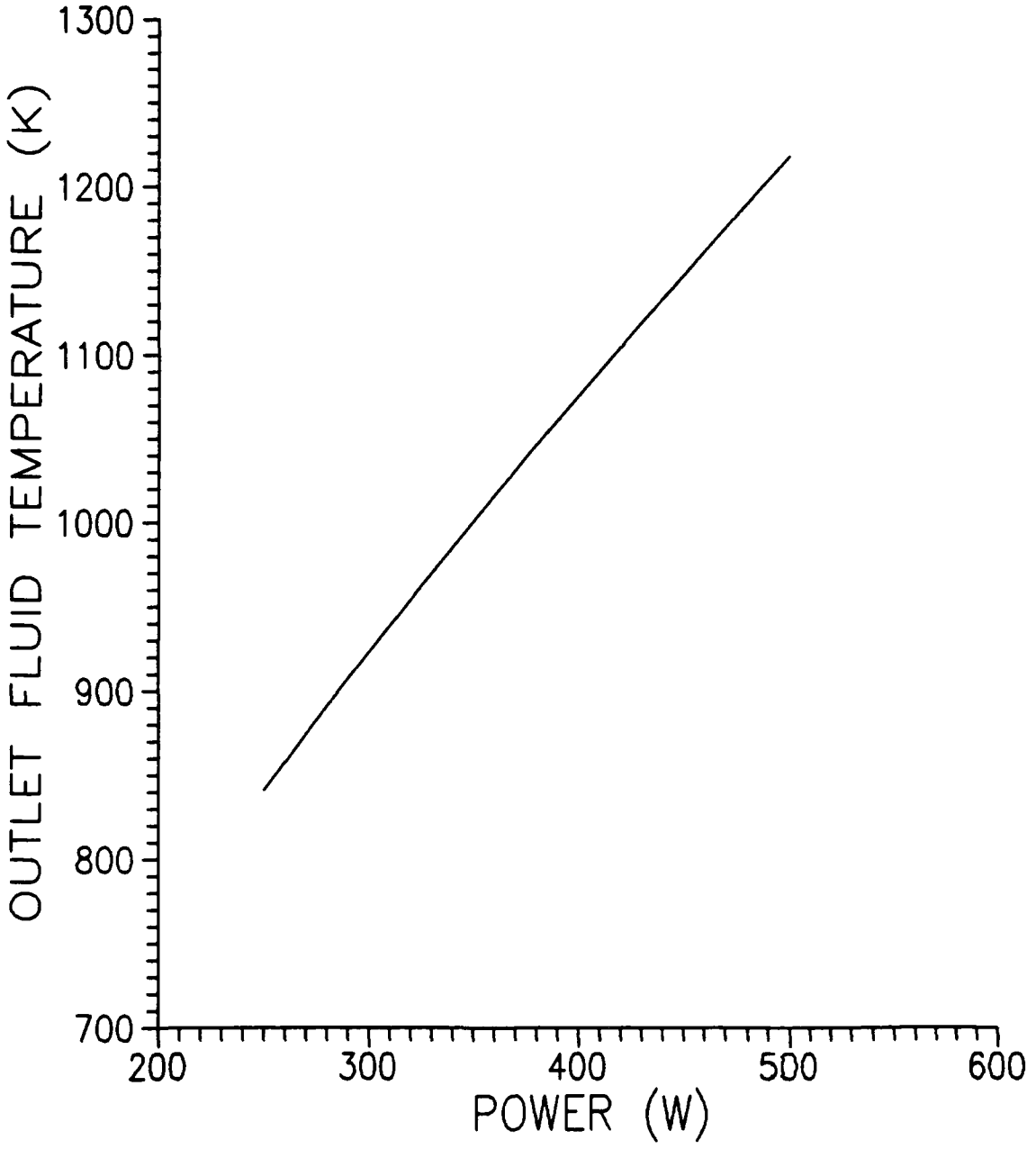

p = 1.5 atm **$\dot{m}$ = 0.35 kg/hr** **t = 100 hrs**

Figure 6-10. Fluid Temperature vs. Power Level

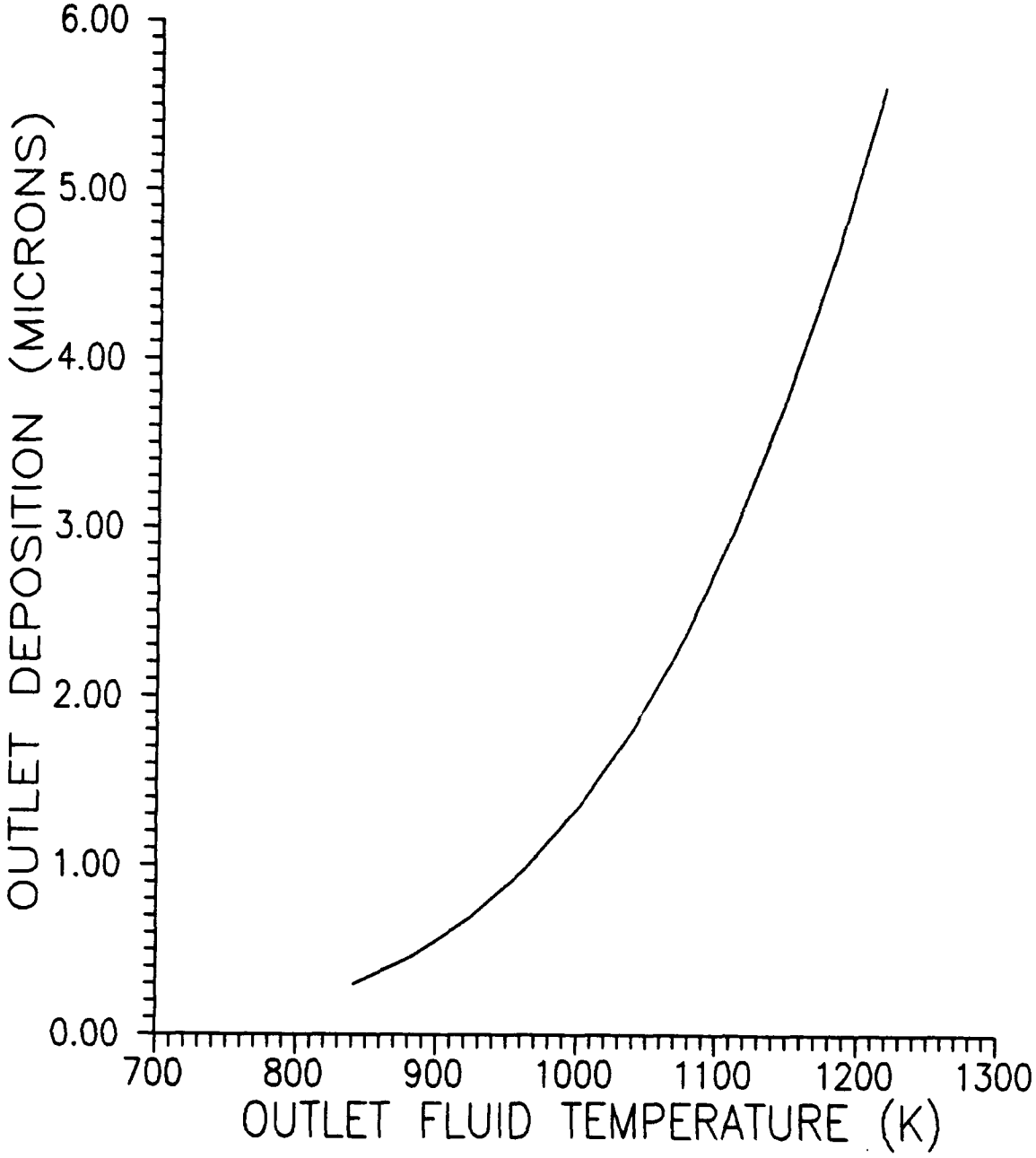

p = 1.5 atm **$\dot{m}$ = 0.35 Kg/hr** **t = 100 hours**

Figure 6-11. Carbon Deposition vs. Fluid Temperature

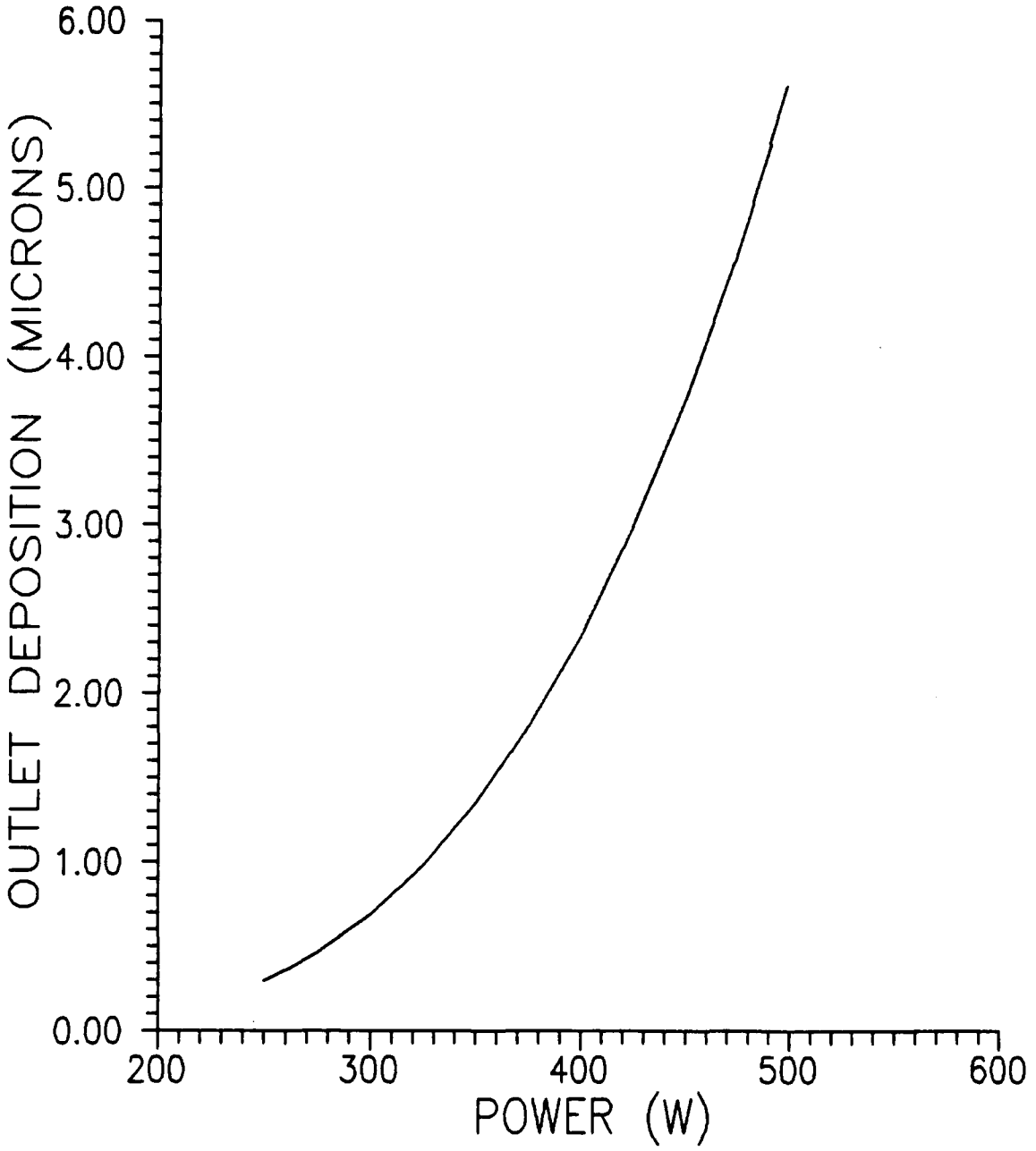

p = 1.5 atm **$\dot{m}$ = 0.35 kg/hr** **t = 100 hours**

Figure 6-12. Carbon Deposition vs. Power Level

Equation 6-2 can be combined with Equation 6-1 to give an expression relating thrust, mass flow rate, and specific impulse:

$$F \cong \dot{m} I_s g_o \qquad (6\text{-}3)$$

Therefore, optimizing the mass flow rate is important to resistojet operation. For a methane propellant, the mass flow rate will also impact the carbon deposition rate. This effect can be studied from two perspectives. The first maintains a constant resistojet power and allows the varying mass flow rate to determine the fluid temperature, and the second varies power with mass flow rate to maintain a constant fluid outlet temperature.

Constant Power

As the mass flow rate is increased in a resistojet at constant power, Equation 4-2:

$$q_f = \dot{m} c_p (\Delta T_m) \qquad (4\text{-}2)$$

shows that if a constant heat transfer rate is maintained, the fluid temperature in the heat exchanger will increase at a lower rate and achieve a lower outlet value. This relationship is shown in Figure 6-13.

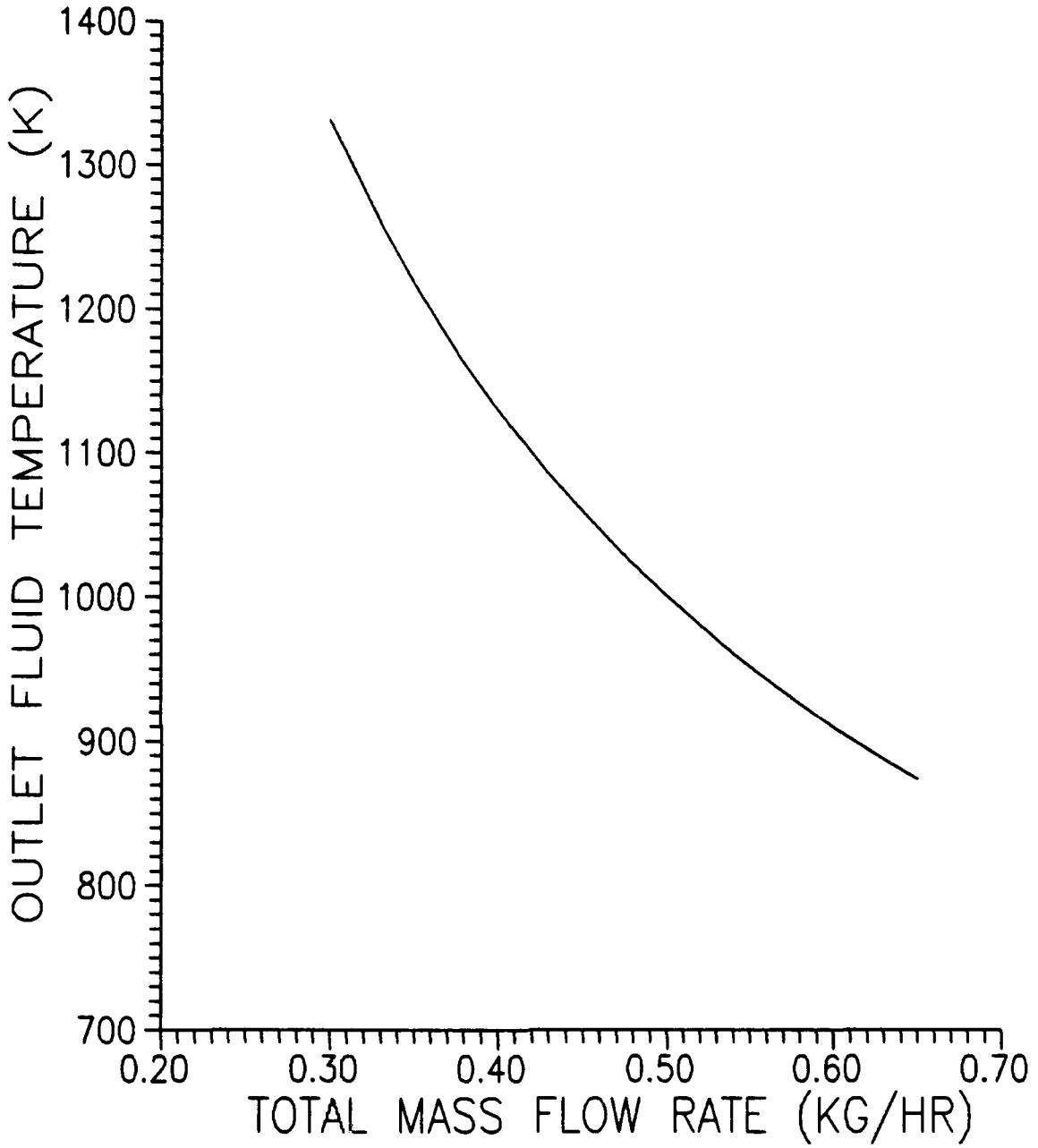

p = 1.5 atm **W = 500 W**

Figure 6-13. Fluid Temperature vs. Mass Flow Rate

These lower temperatures result in a lower carbon deposition rate from methane. A higher mass flow rate at constant pressure also increases the fluid velocity, dropping the residence time of methane in the heat exchanger, and reducing the radical species produced. The combination of these factors is illustrated in Figure 6-14.

Constant Temperature

If the heat exchanger outlet fluid temperature is kept constant, the resistojet power required to attain that temperature varies approximately linearly with the mass flow rate, as shown in Figure 6-15. At lower mass flow rates, Equation 4-2 shows that the fluid will rise to higher temperatures. The lower fluid velocity that accompanies a lower mass flow rate also increases the methane residence time in the heat exchanger. This combination allows the heat exchanger to raise the fluid to the desired temperature for less power.

At lower mass flow rates, the fluid is also brought to a temperature near the channel surface temperature much sooner in the heat exchanger channel. This change in fluid temperature profile is shown in Figures 6-16 and 6-17.

Methane at low mass flow rates, then, is elevated to a high temperature sooner, and spends more time in the exchanger channel than at high mass flow rates.

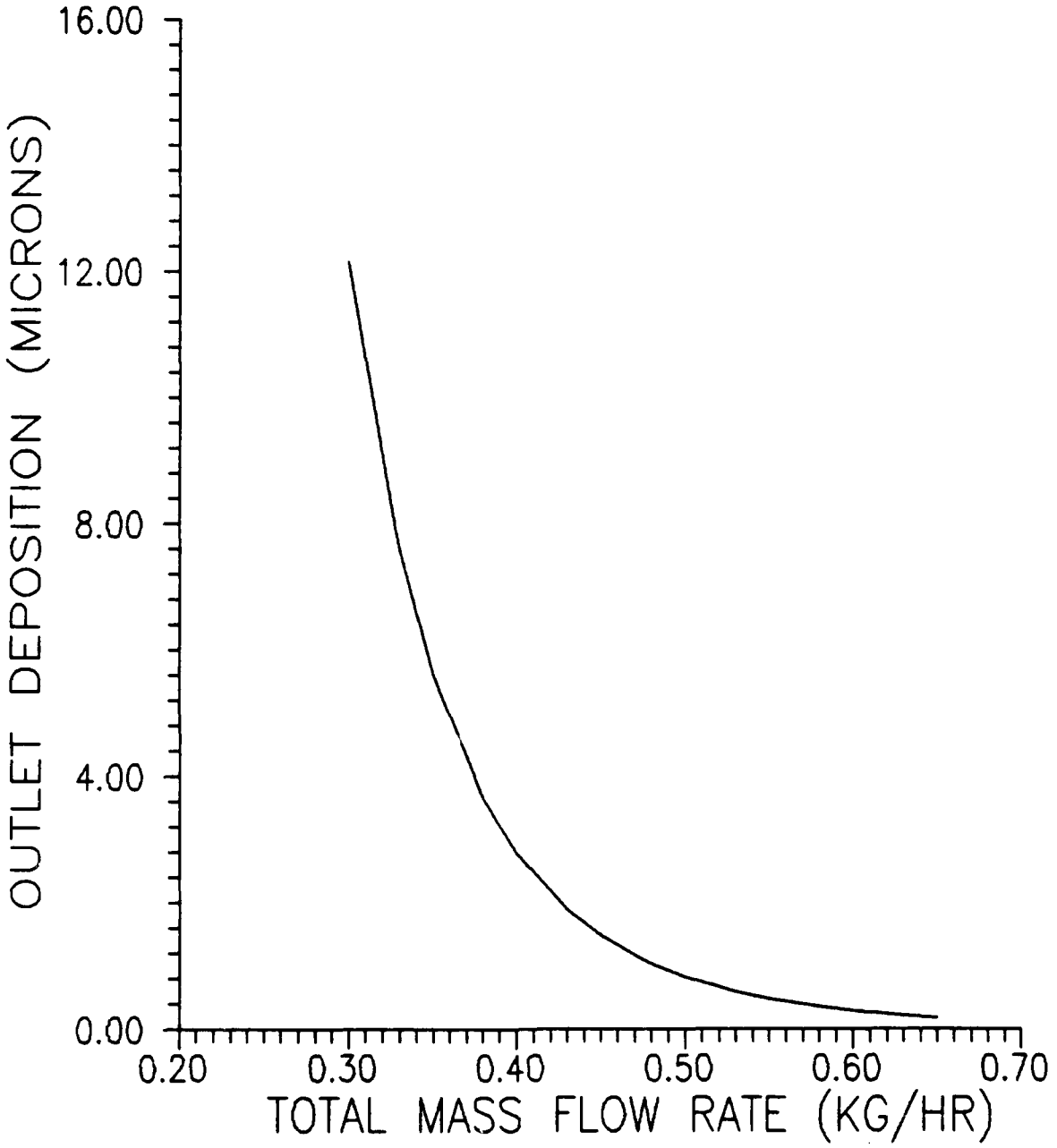

p = 1.5 atm W = 500 W t = 100 hours

Figure 6-14. Carbon Deposition vs. Mass Flow Rate at Constant Power

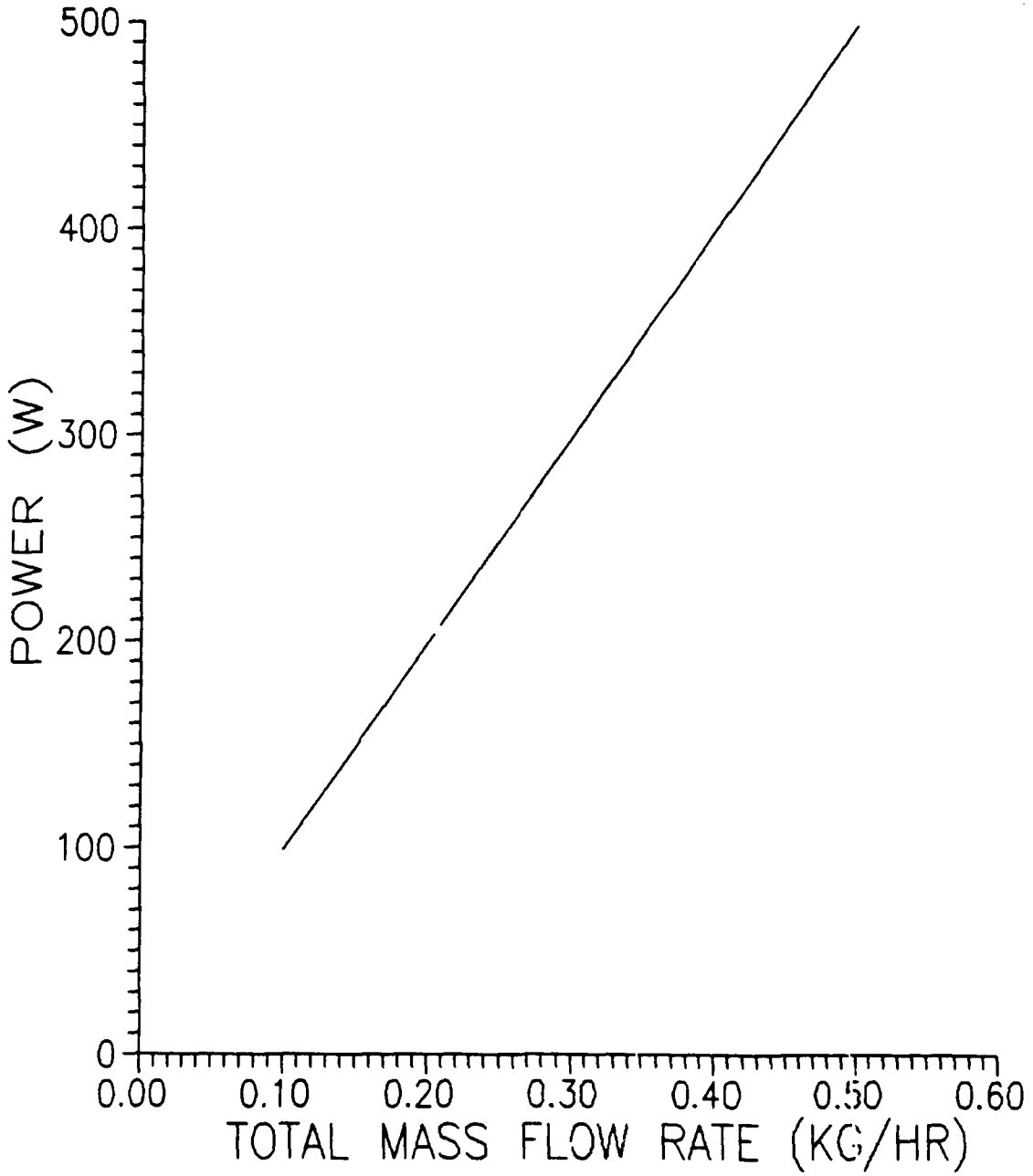

$p = 1.5$ atm $\quad T_c = 1000$ K

Figure 6-15. Power Level vs. Mass Flow Rate

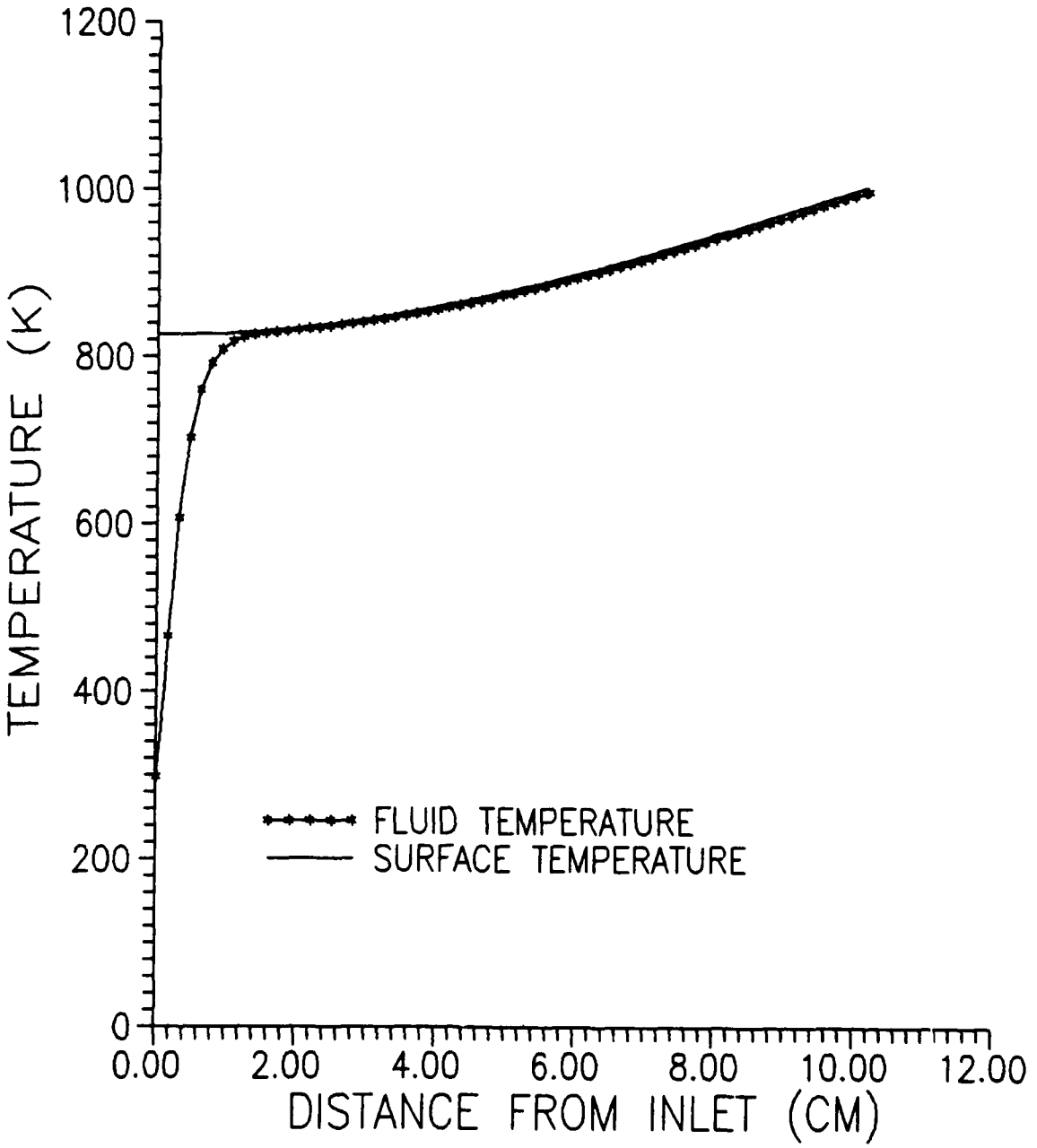

p = 1.5 atm T_c = 1000 K $\dot{m}$ = 0.2 Kg/hr

Figure 6-16. Heat Exchanger Temperature Profile for a Lower Mass Flow Rate

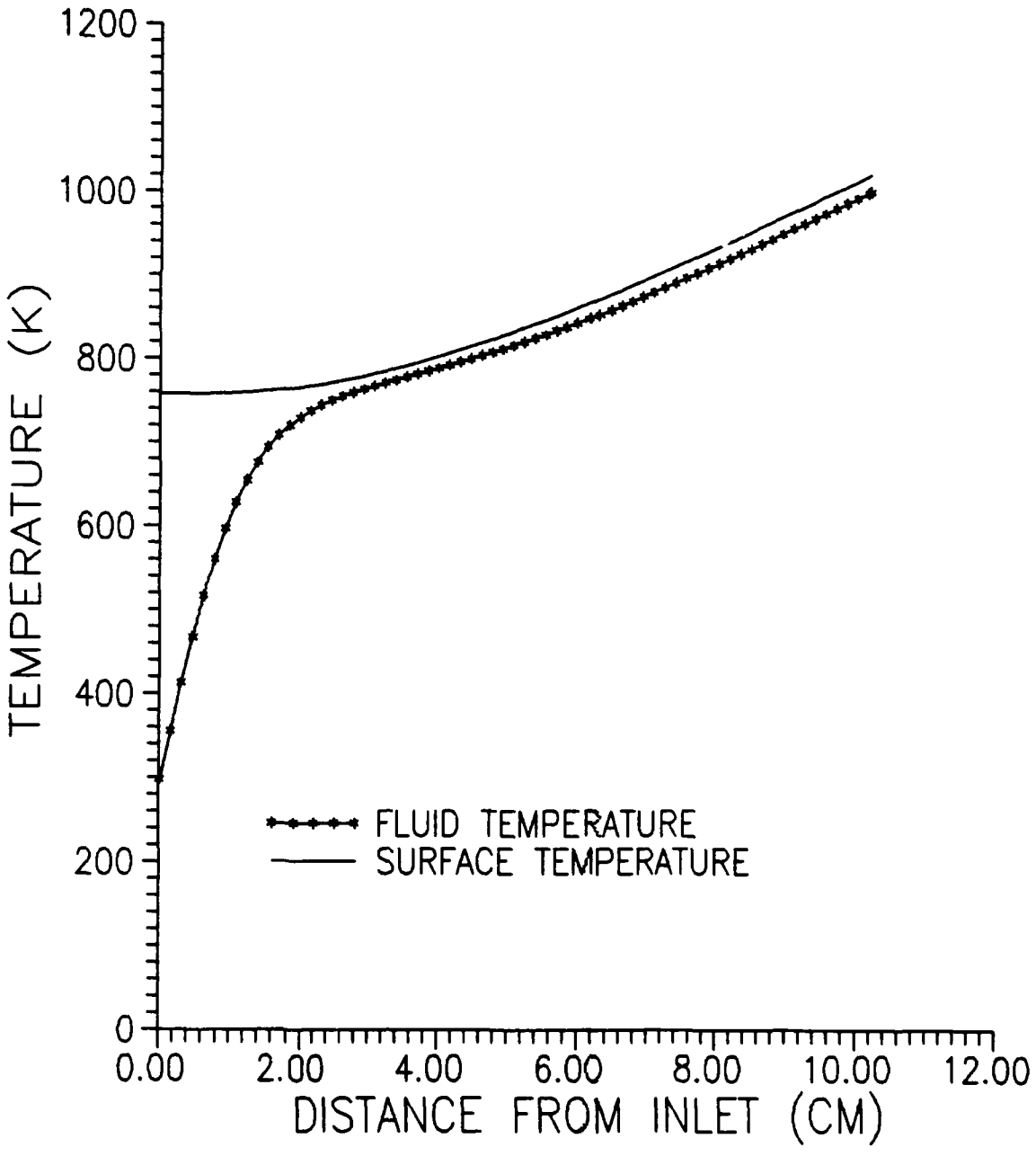

p = 1.5 atm **T_c = 1000 K** **$\dot{m}$ = 0.5 Kg/hr**

Figure 6-17. Heat Exchanger Temperature Profile for a Higher Mass Flow Rate

Consequently, the carbon deposition rate increases greatly at low mass flow rates at fixed exit temperatures, similar to the increase at fixed power. This relationship is shown in Figure 6-18.

The effect of mass flow rate on carbon deposition for methane indicates that optimizing the flow rate and specific impulse will require an additional consideration for deposition. The higher deposition rates found at lower mass flow rates need to be evaluated when determining optimum resistojet operating conditions with methane.

Nozzle Performance

While the program indicates that the deposition of carbon does not immediately effect the performance of the resistojet heat exchanger, deposition in the resistojet nozzle could cause an immediate loss in its efficiency. The difficulty in analyzing the resistojet nozzle is that its performance is not constant versus temperature.

Nozzle performance, described by the propellant exit velocity, can be calculated several different ways. If the nozzle flow is assumed to be isentropic, the exit velocity of the propellant may be found from the change in propellant molecular enthalpy (29:40):

$$V_e = [2(h_c - h_e)]^{1/2} \qquad (6\text{-}4)$$

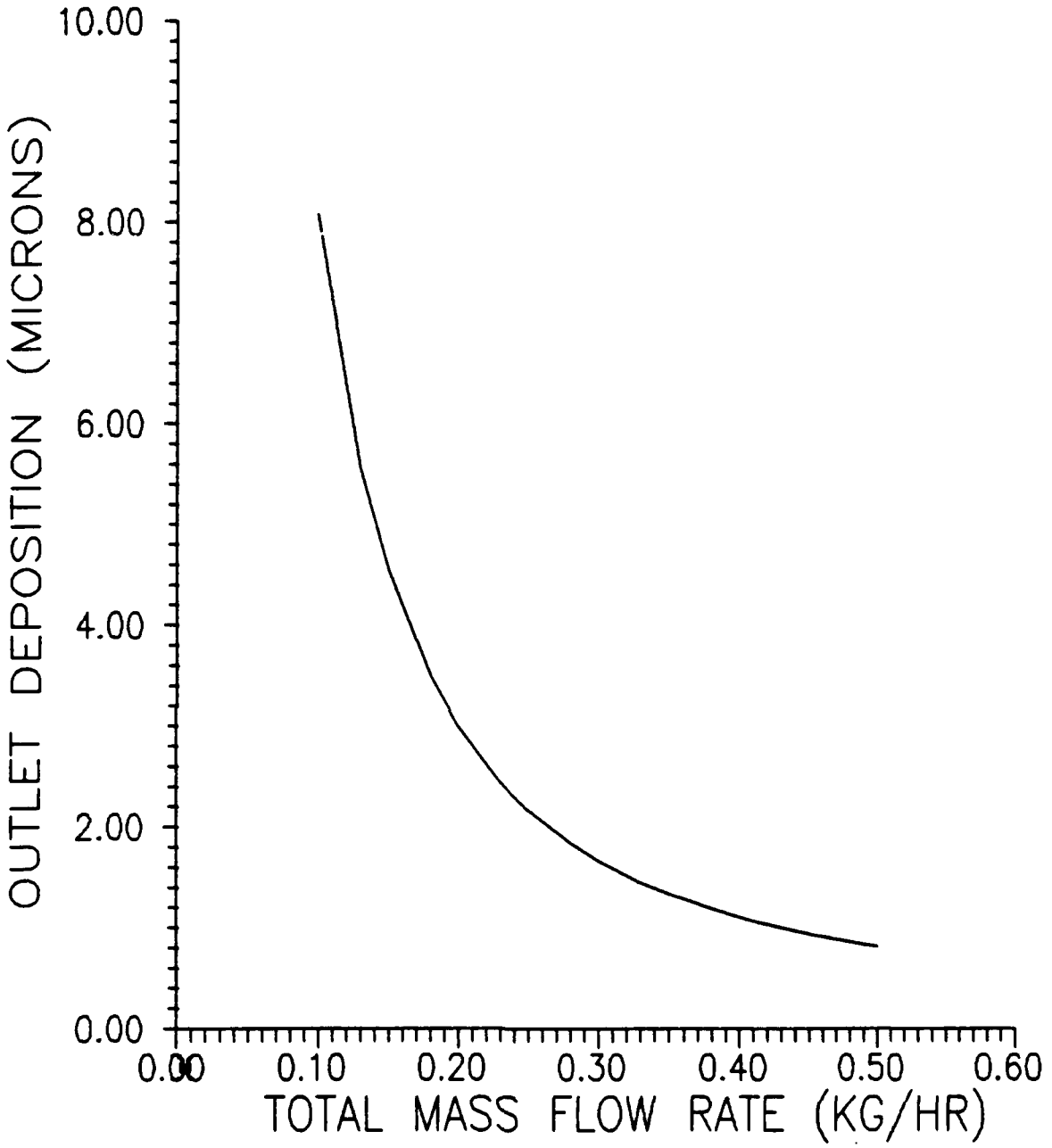

p = 1.5 atm **T_c = 1000 K** **t = 100 hours**

Figure 6-18. Carbon Deposition vs. Mass Flow Rate at Constant Outlet Temperature

where h_c is the heat exchanger exit (chamber) molecular enthalpy, and h_e is the exit enthalpy.

Because the propellant flow in a resistojet is essentially pure, the values for enthalpy can be easily obtained from the chamber and exit temperatures. If the exit temperature is not known, it can be found by balancing the entropy for the nozzle flow from the equation (2:62-65):

$$S_c^\circ - S_e^\circ = R\ln(p_c/p_e) \tag{6-5}$$

where S_c° and S_e° are the chamber and exit standard entropies, R is the gas constant, and p_c and p_e are the chamber and exit pressures.

The exit pressure can be defined from the gas law:

$$p_e = \rho_e R T_e \tag{6-6}$$

and conservation of mass:

$$\rho_e = \dot{m}/A_e V_e \tag{6-7}$$

where ρ_e is the gas exit density, and A_e is the nozzle exit area.

By iterating around Equations 6-4 through 6-7, nozzle conditions can be determined, and the specific impulse found by Equation 6-1.

If the thermodynamic properties of the propellant remain relatively constant through the nozzle, the exit velocity can be solved directly as a function of the propellant ratio of specific heats (γ), the chamber temperature, and the chamber and nozzle exit pressures (29:40):

$$V_e = \left[\frac{2\gamma R}{(\gamma - 1)M} T_c \{1 - (p_e/p_c)^{\gamma-1/\gamma}\}\right]^{1/2} \qquad (6\text{-}8)$$

where R is the universal gas constant, and M is the propellant molecular weight.

If the exit pressure is very small when compared to the chamber pressure, the pressure term can be omitted, and Equation 6-8 reduces to (25):

$$V_e = \left[\frac{2\gamma R}{(\gamma - 1)M} T_c\right]^{1/2} \qquad (6\text{-}9)$$

where γ is a function of temperature and assumed constant. In reality γ changes with propellant temperature through the nozzle, and this introduces inaccuracies into nozzle calculations, as shown below.

If experimental data from LRC on the engineering model resistojet is used in Equations 6-4 and 6-9, and the results converted to specific impulse by Equation 6-1, the calculated ideal specific impulse values can be compared to the measured specific impulse results. An assessment of how

well the nozzle conforms to ideal operation can then be made.

Such an assessment shows that the engineering model resistojet performance varies far from calculated ideal conditions. To correct for this variation, LRC has relied on an empirically modified version of Equation 6-9 to predict resistojet performance (3:15):

$$I_s = CF\frac{T_c}{M}^{1/2} \qquad (6\text{-}10)$$

where CF is an empirical correction factor that varies for each propellant type.

Computed values for resistojet specific impulse from Equations 6-4, 6-9, and 6-10 are compared to experimental results from the resistojet in Table 6-2.

The discrepancy between calculated and measured specific impulse is partially due to the change in propellant physical properties like the specific heat ratio, and partially due to mechanical inefficiencies in the nozzle. Detailed analysis of the effects of carbon deposition in the nozzle will be difficult until an accurate description of nozzle performance over different temperatures and propellants is obtained. However, the general effects can be estimated using the principles of this investigation.

Table 6-2. Comparison of Computed and Measured Resistojet Specific Impulse (3:14)

Chamber Temperature (K)	Specific Impulse (sec) Measured	Eq. 6-4	Eq. 6-9	Eq. 6-10
303	72	72.9	80.9	70.2
773	112	124.4	134.2	112.1
1173	139	158.0	170.8	138.1
1473	154	180.3	196.0	154.8

The heat exchanger analysis program computes a methane temperature and radical concentration as the propellant enters the chamber. The resistojet plans can be used to estimate a residence time for methane in the chamber, from which the deposition on the chamber wall and the radical concentration at the nozzle entrance can be computed. For the nozzle, the fully developed laminar flow analysis of the heat exchanger can be replaced by a one dimensional flow analysis. From this, incremental changes in the fluid temperature, radical concentration, and carbon deposition

can be calculated, and nozzle throat and exit conditions determined.

An estimate of the carbon deposition in the nozzle can be made if nozzle flow is assumed to be ideal and isentropic. For the flow conditions initially performed for this heat exchanger ($\dot{m}$ = 0.35 kg/hr, W = 500 W, p = 1.5 atm), the methane chamber temperature is 1218 K, and the radical concentration is 9.17 x 10^{-2} mmole/l. The nozzle throat temperature can be estimated from the propellant temperature and specific heat ratio values at the heat exchanger outlet by the equation (29:44):

$$T_t = 2T_c/(\gamma + 1) \qquad (6\text{-}11)$$

and for this example is equal to 1150 K.

The cross sectional area to perimeter ratio for nozzle throat is 0.0255 cm, comparable to the heat exchanger channel, and the channel value for the fraction of depositing radicals (α) for the heat exchanger can be substituted. Applying Equations 4-27 through 4-29 gives a carbon deposition rate at the throat of 0.067 μm/hr.

The effect of this deposition can be measured by nozzle flow theory. The gas velocity at the throat (V_t) will always be sonic, and the flow rate will change with deposition to maintain this condition. The throat velocity is given by the equation (29:45):

$$V_t = (\gamma R T_t)^{1/2} \qquad (6\text{-}12)$$

The pressure at the throat (p_t) will be a function of the heat exchanger outlet pressure (29:44):

$$p_t = p_c\left[\frac{2}{\gamma + 1}\right]^{\gamma/\gamma-1} \qquad (6\text{-}13)$$

The gas density at the throat can be found from the universal gas law:

$$\rho_t = p_t/RT_t \qquad (4\text{-}20)$$

The throat area (A_t) will decrease with the carbon deposition, and the resulting mass flow rate can be found by:

$$\dot{m} = \rho_t A_t V_t \qquad (6\text{-}14)$$

If Equation 6-10 is used to calculate the resistojet specific impulse, and Equation 6-3 to then compute the resulting thrust, an analysis of the resistojet performance over time can be made. The effects of nozzle deposition for this example are shown in Table 6-3.

Table 6-3. Resistojet Performance with Carbon Deposition in the Nozzle Throat

Time of Operation (hours)	Throat Area ($m^2 x 10^{-7}$)	Mass Flow Rate (Kg/hr)	Thrust (mN)	Drop in Thrust (%)
0	8.17	0.350	187	0
50	8.06	0.348	186	1
100	7.96	0.343	184	2
500	7.15	0.308	165	12
1000	6.22	0.268	143	24
1500	5.35	0.230	123	34
2000	4.63	0.198	106	43

Inlet p = 1.5 atm W = 500 W $\dot{m}$ = 0.35 Kg/hr

Table 6-3 illustrates the impact carbon deposition can have on resistojet performance. Although deposited carbon will not greatly change the heat exchanger performance, its effect on nozzle performance means that deposition in the resistojet should be minimized.

Since maintenance on the resistojet is not desirable, control of carbon deposition must be done remotely, and may be done by either of two means. First, operation of the resistojet with methane can be optimized to obtain the highest thrust and specific impulse values while keeping the carbon deposition rate within an acceptable level. The heat exchanger analysis program developed in this investigation, if extended to the resistojet nozzle, could provide an excellent means to determine such an optimum operating level.

Carbon deposition in the resistojet could also be controlled by alternating propellants between methane and gases that can strip deposited carbon from the heat exchanger channels and resistojet nozzle, like oxygen or water. This type of operation could allow for higher operating conditions with methane, improving its benefit as a propellant. If equations can be developed to describe the removal of carbon by a stripping gas in the resistojet, then the principles of this investigation could again by applied to determine the effects of these gases over time in the resistojet under a variety of carbon deposition conditions.

VII. Conclusions and Recommendations

The engineering model resistojet heat exchanger analysis program developed in this investigation predicts resistojet characteristics that match experimental results for methane and carbon dioxide in the 800-1200 K chamber temperature range. The program may also be adapted toward the use of any proposed resistojet propellant by including the proper values of propellant specific heat, viscosity, and thermal conductivity.

The program shows that carbon deposition from methane varies along the length of the heat exchanger, and also shows the variation of this deposition with operational pressure, power, and mass flow rate. The performance of the heat exchanger does not change greatly with deposition, but analysis of the nozzle indicates that resistojet performance would be significantly affected by carbon deposition, and the minimization of carbon deposition is a key factor for methane operation.

The work of this investigation may be extended in a variety of ways. The program may be extended to include the resistojet nozzle by including an accurate analysis of the nozzle performance. The carbon deposition model may be improved by developing an expression for the fraction of depositing molecules (α) based on kinetic theory and adaptable for any channel, rather than using a value for α

derived from one set of experimental results. Resistojet operation may be optimized for methane between mass flow rate, specific impulse, and the carbon deposition rate. The program may also be extended to examine the operation of the resistojet with gas mixtures. Finally, the program may be adapted to study the use of gases like oxygen and water vapor, alternating with methane to remove deposited carbon from the resistojet interior.

Appendix A: Heat Exchanger Analysis Results at 1.5 Atm Pressure

W = 500 W $\dot{m}$ = 0.35 kg/hr

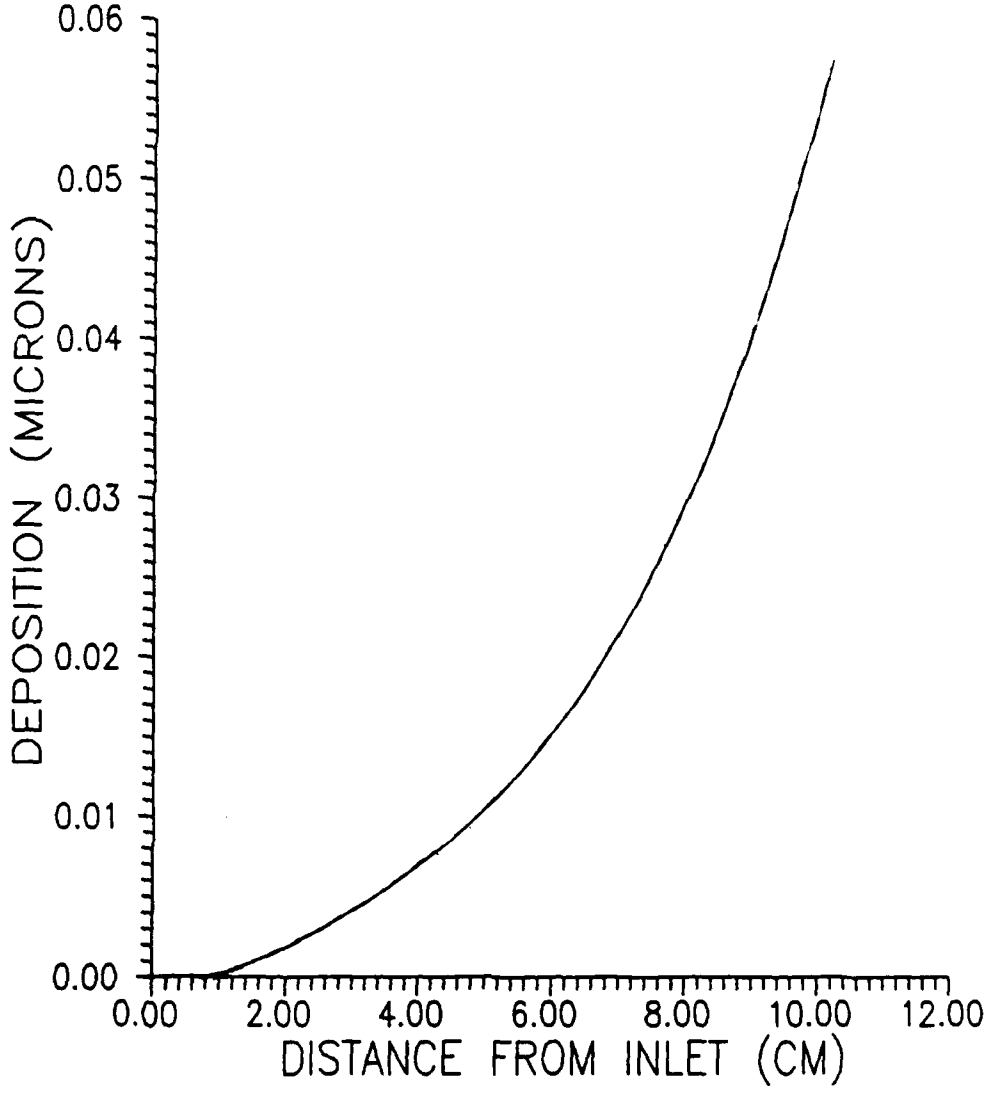

Figure A-1. Carbon Deposition at 1 Hour

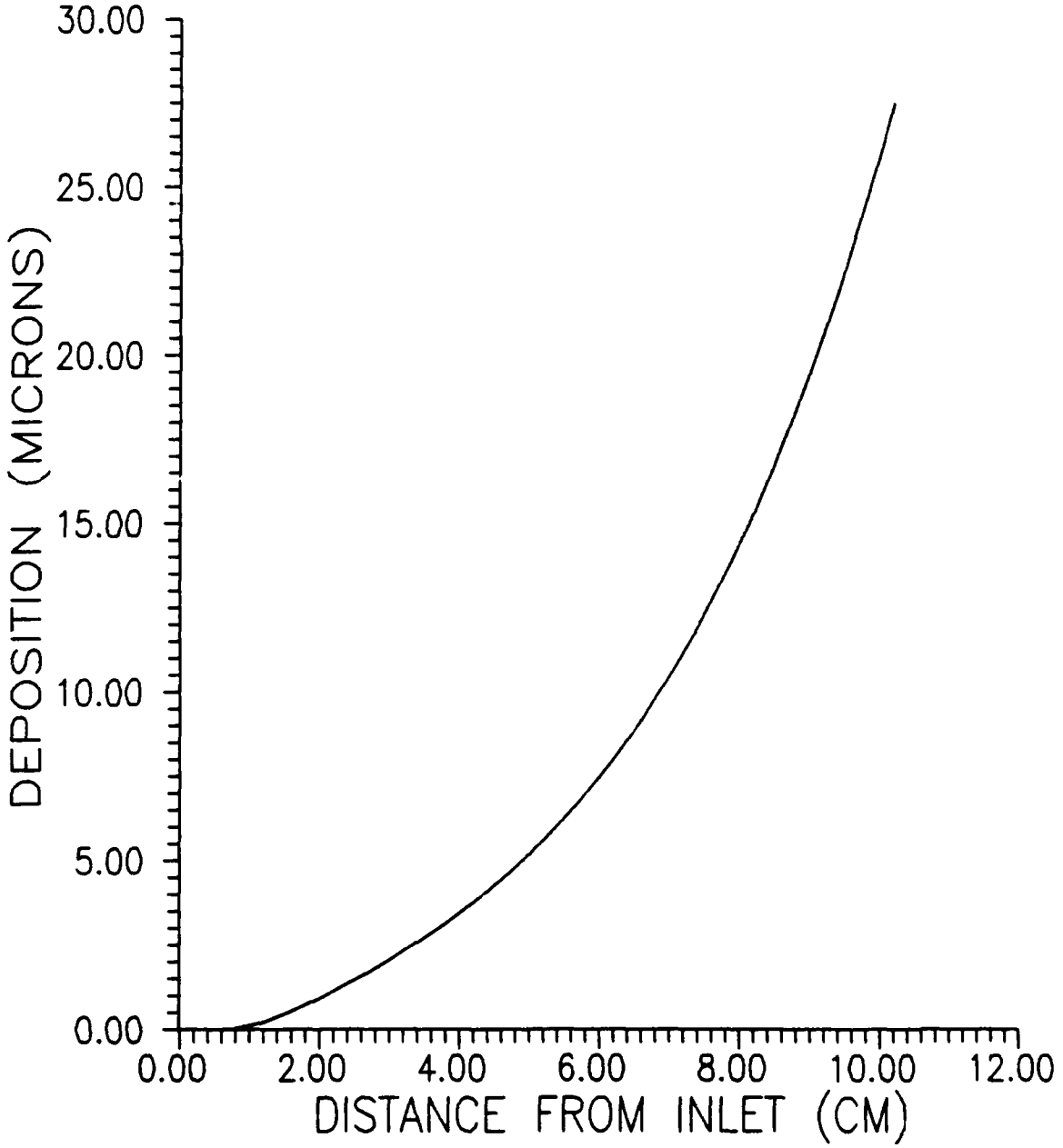

Figure A-2. Carbon Deposition at 500 Hours

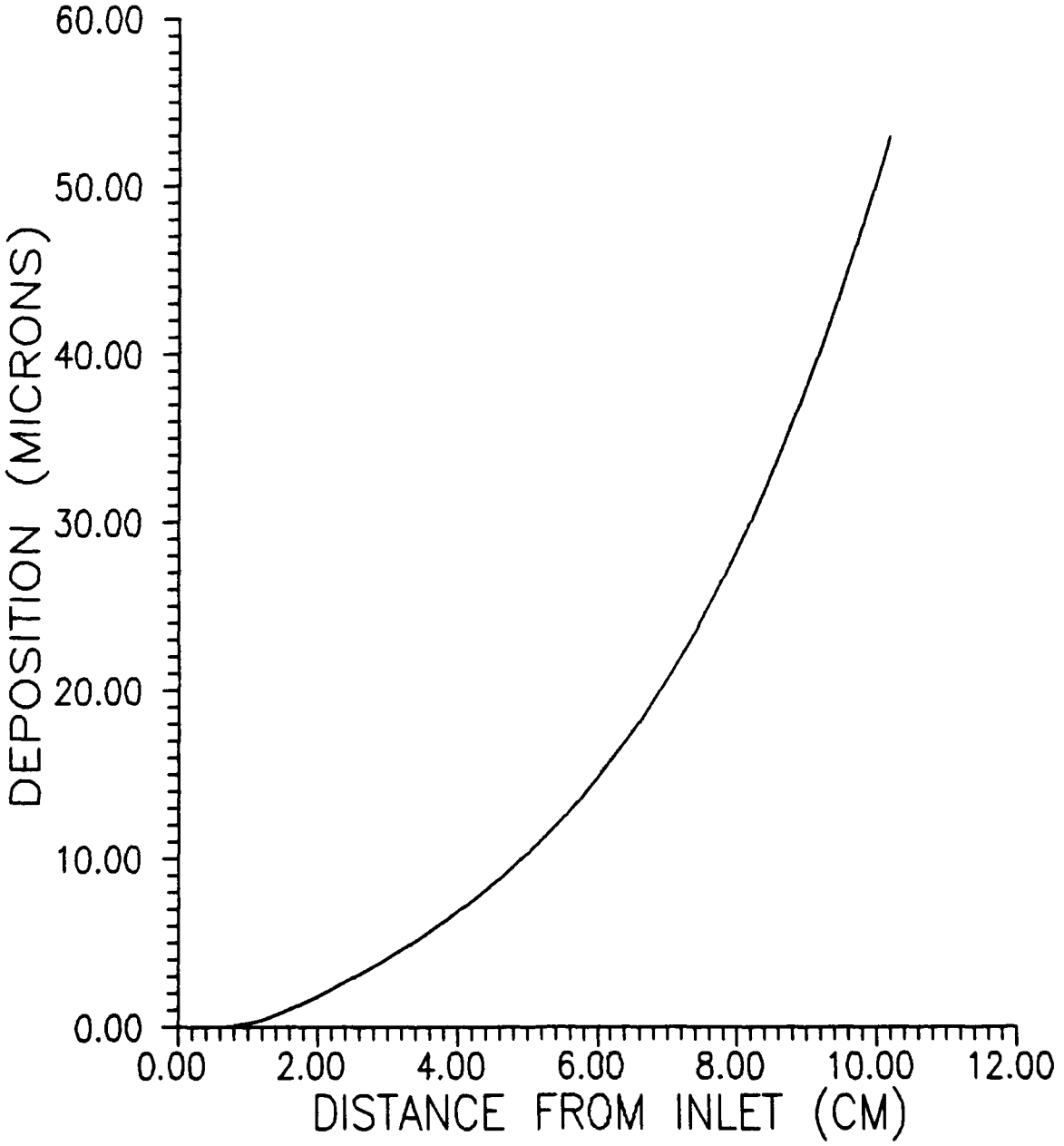

Figure A-3. Carbon Deposition at 1000 Hours

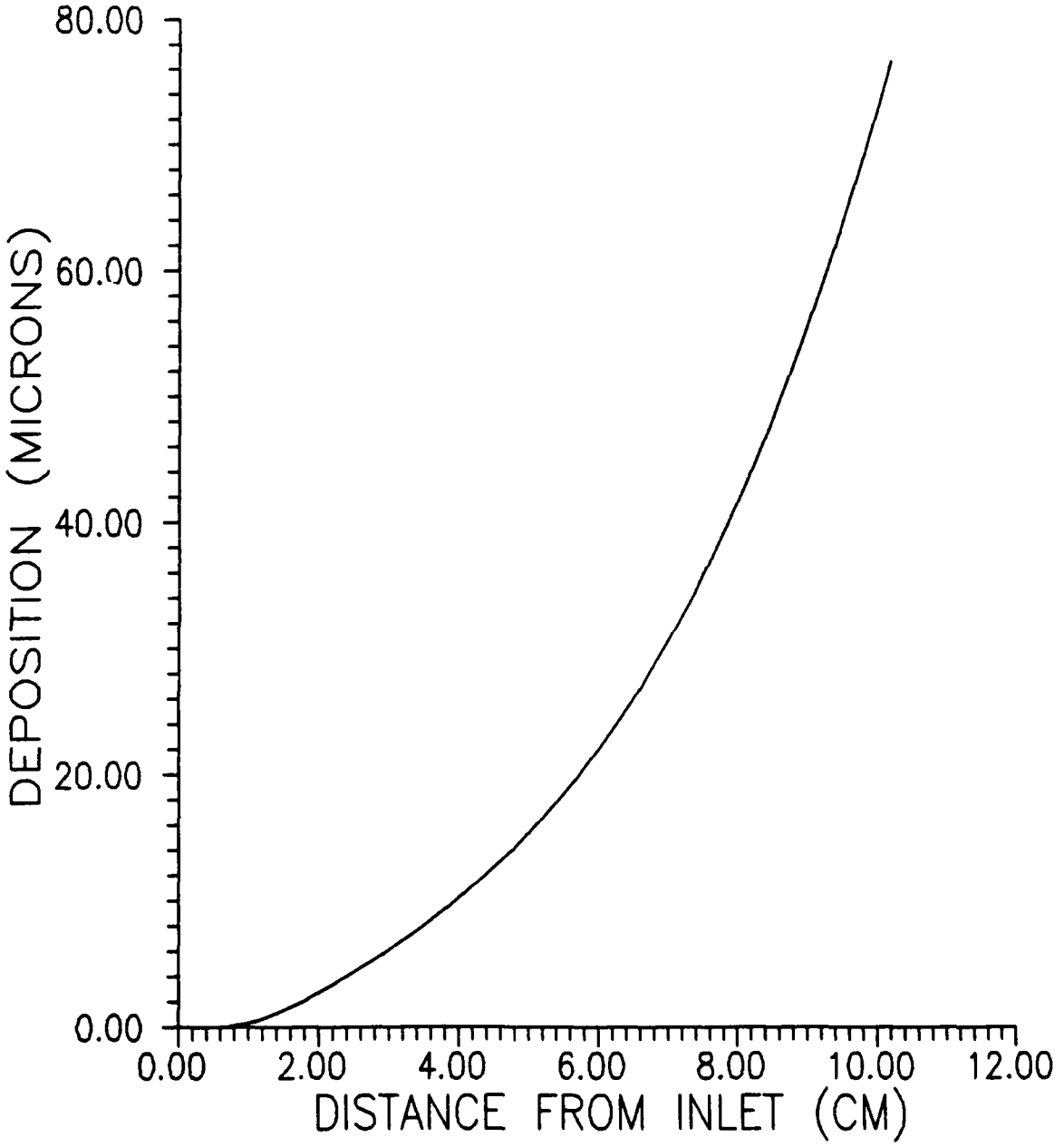

Figure A-4. Carbon Deposition at 1500 Hours

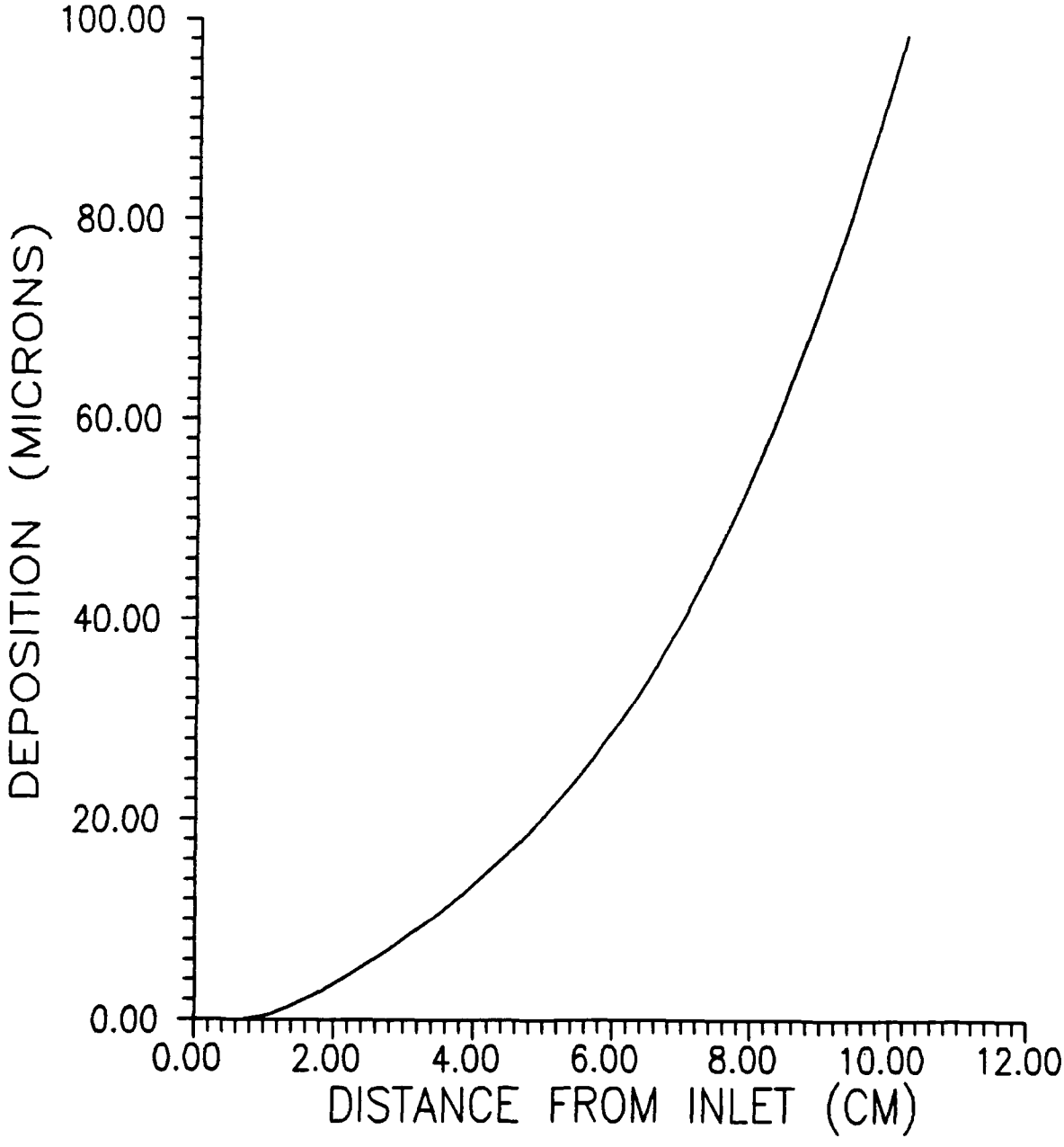

Figure A-5. Carbon Deposition at 2000 Hours

Appendix B: Heat Exchanger Analysis Results at 3 Atm Pressure

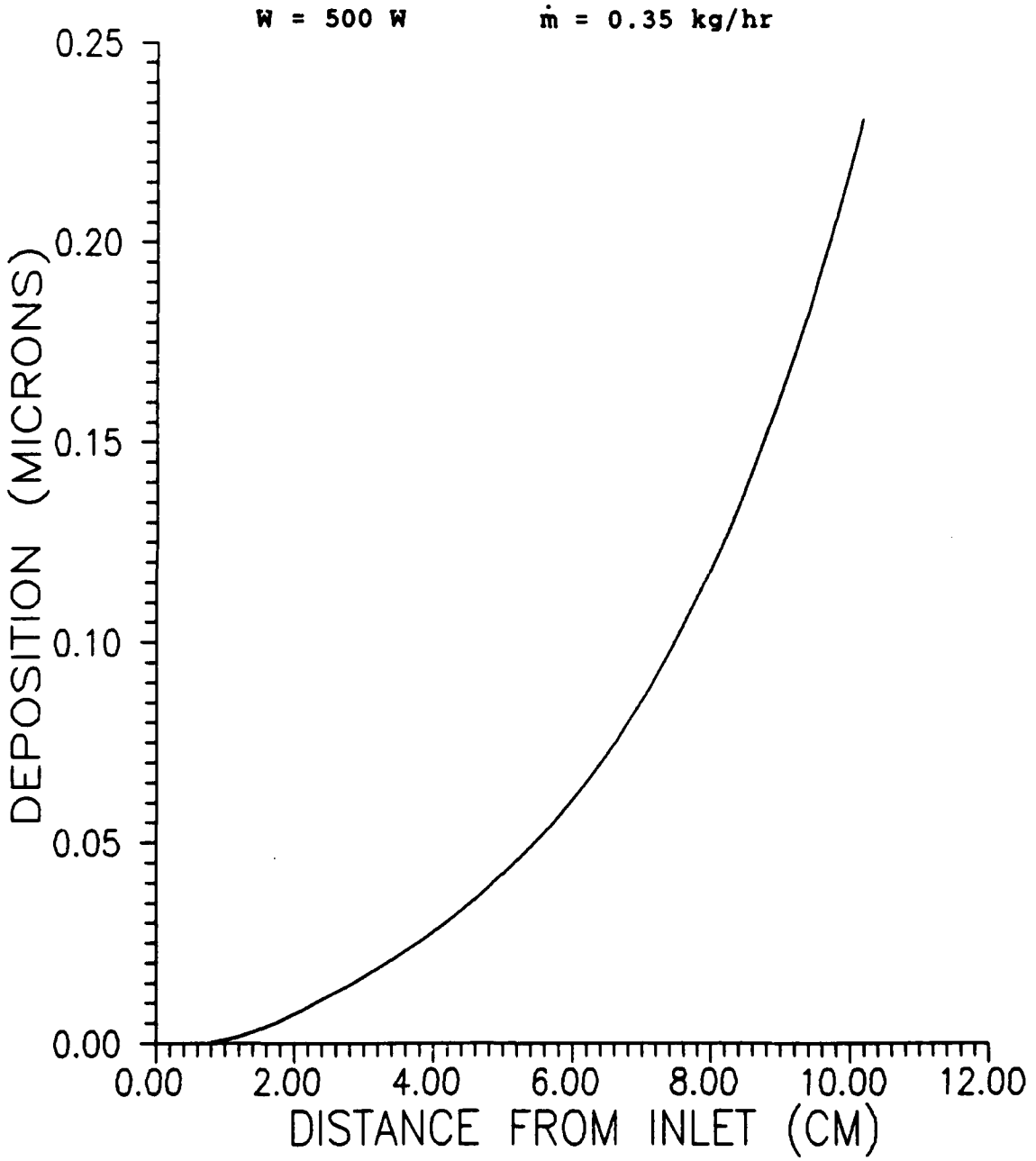

Figure B-1. Carbon Deposition at 1 Hour

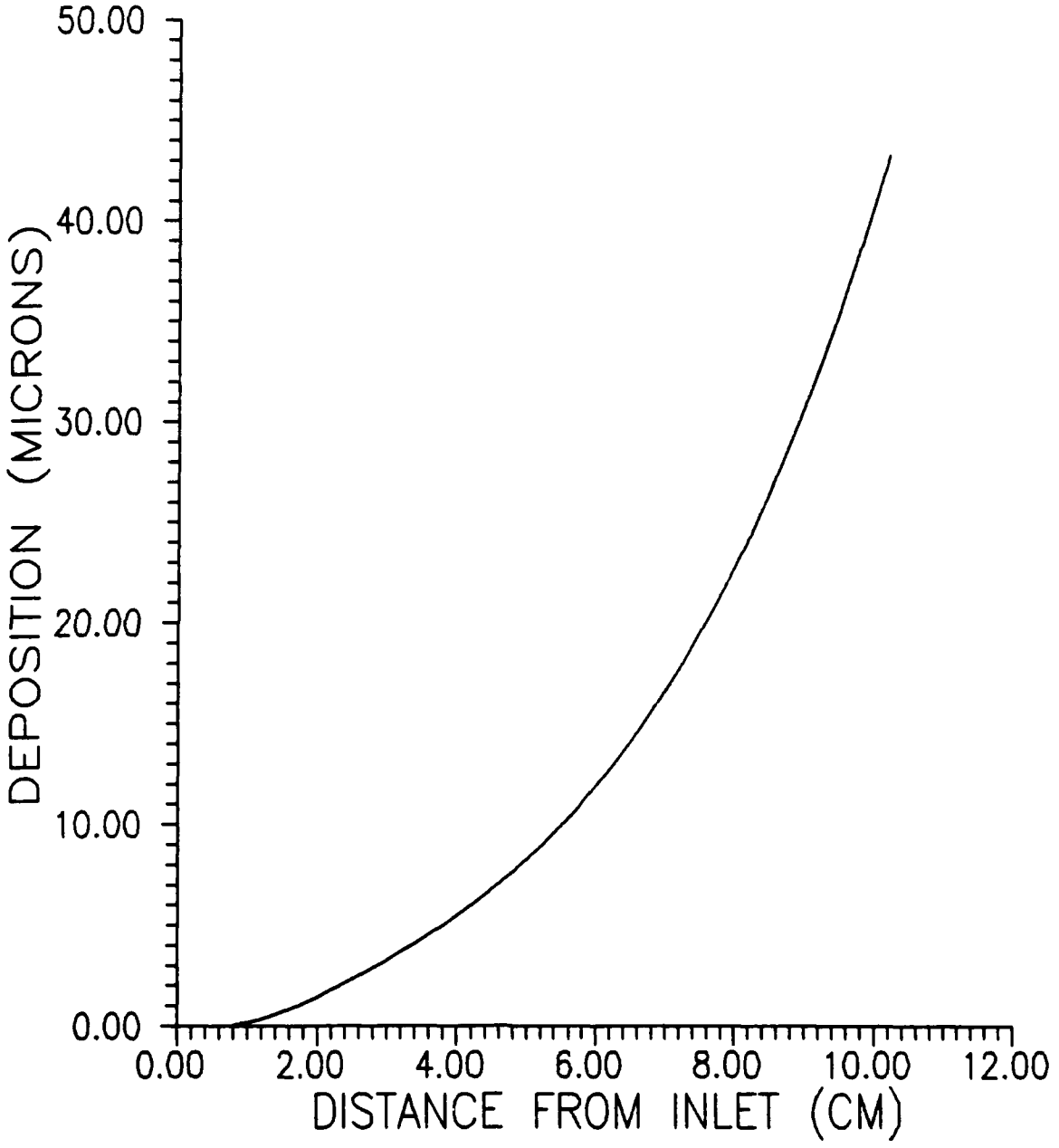

Figure B-2. Carbon Deposition at 200 Hours

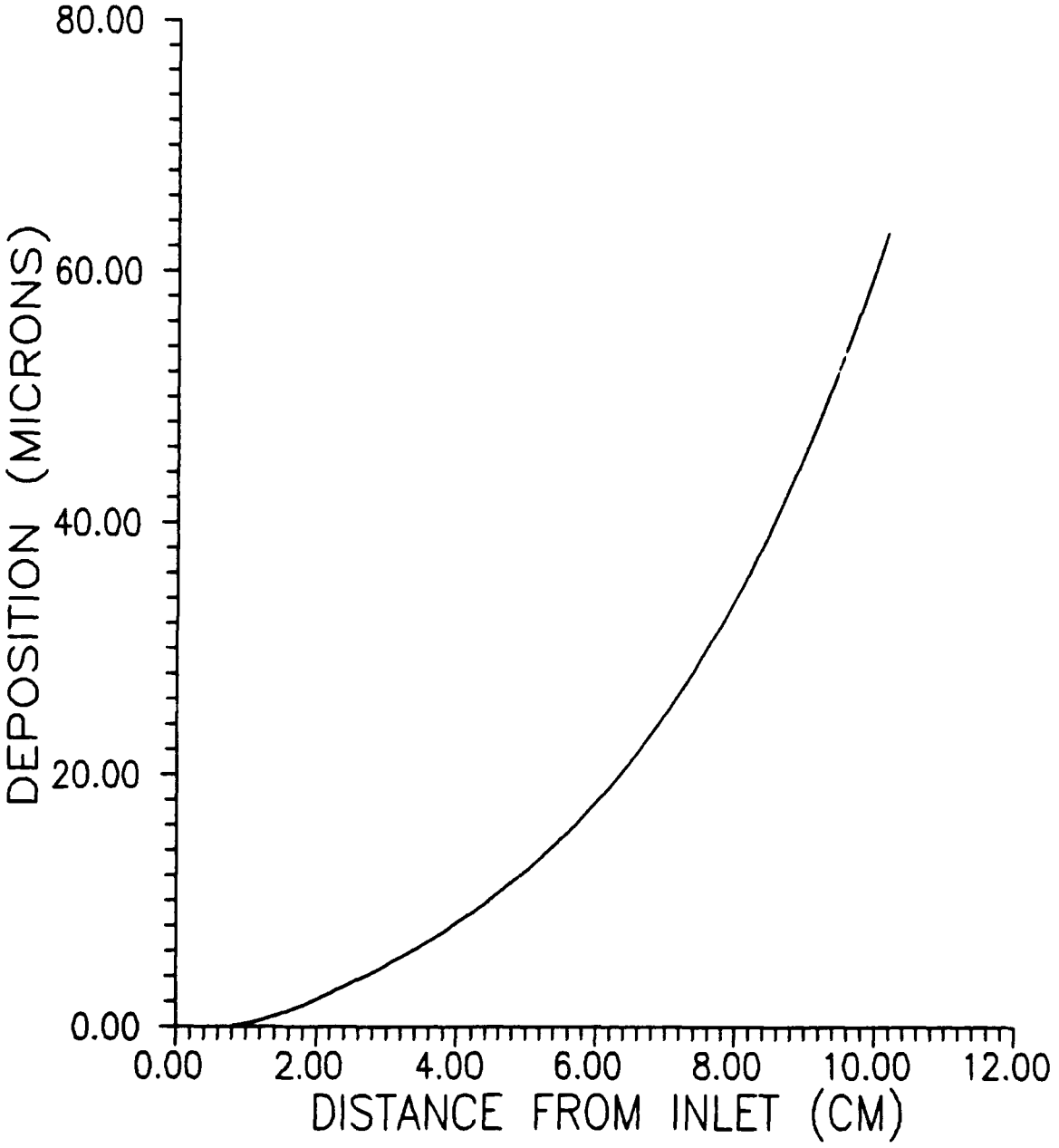

Figure B-3. Carbon Deposition at 300 Hours

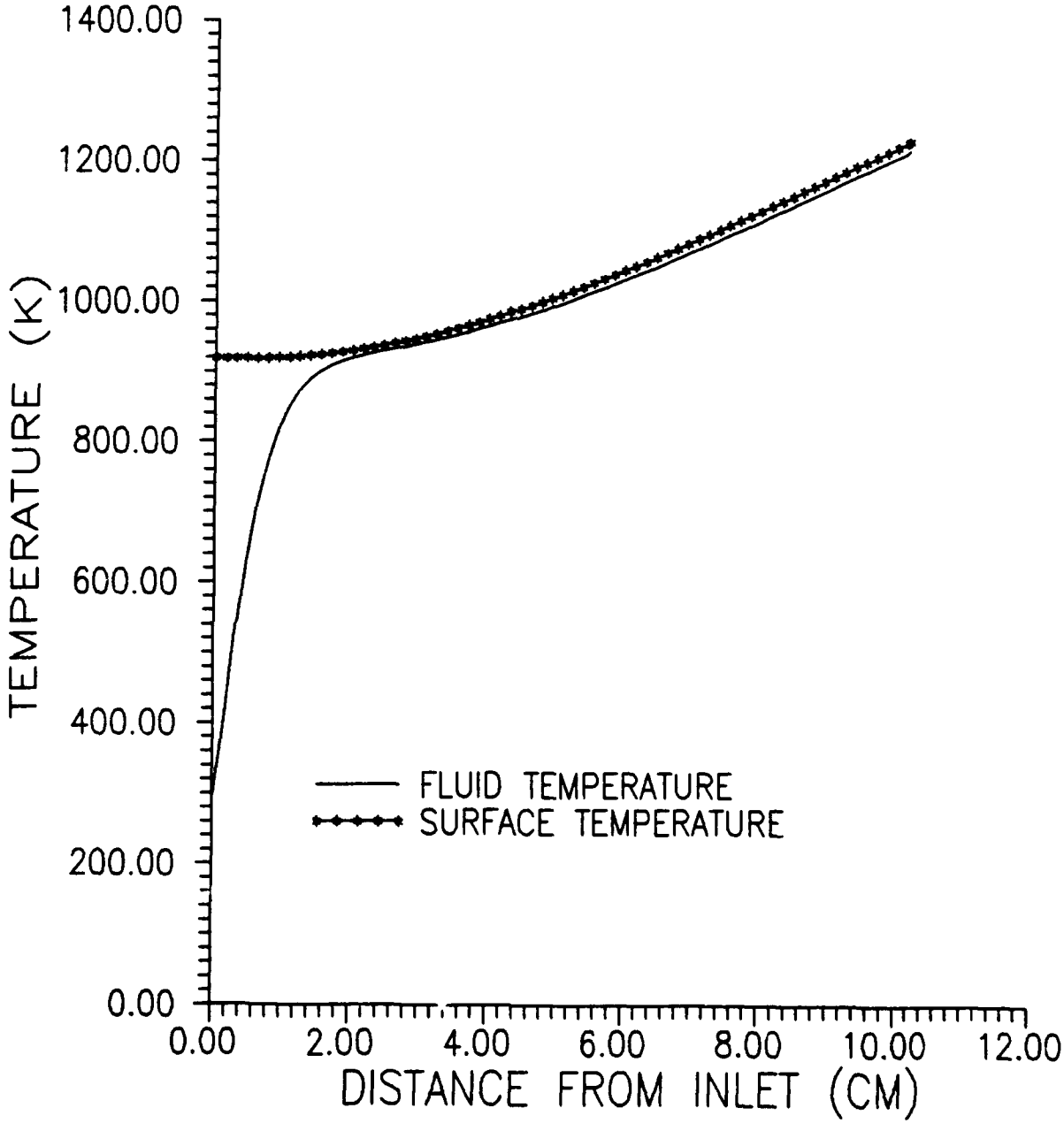

Figure B-4. Fluid Temperature Profile

Appendix C: Heat Exchanger Analysis Program

```
C******RESISTOJET HEAT EXCHANGER ANALYSIS PROGRAM*********
C
C    THIS PROGRAM WILL TAKE A SET OF INLET CONDITIONS FOR THE
C    ENGINEERING MODEL RESISTOJET USING METHANE OR CARBON
C    DIOXIDE AND DETERMINE OUTLET CONDITIONS, INCLUDING
C    CARBON DEPOSITION OVER TIME
C
C    DIMENSION PARAMETERS FOR THE HEAT EXCHANGER=F(X,T)
C    X=DOWNSTREAM DISTANCE     T=OPERATING TIME
       DIMENSION DEP(1000,600),TM(1000,600),P(1000,600)
       DIMENSION A(1000,600)
       DIMENSION TS(1000),H(1000),RN(1000)
       DIMENSION DPT(1000),QD(1000)
C
C    DIMENSION PARAMETERS FOR PROPELLANT PHYSICAL PROPERTIES
C    TO BE READ OFF OF DATA FILES
       DIMENSION TCO2(30),TCO22(30),TCO23(30)
       DIMENSION TCH4(30),TCH42(30),TCH43(30)
       DIMENSION TC(30),CA(30),TP(30),PK(30)
       DIMENSION CPPCO2(30),YKCO2(30),VICO2(30)
       DIMENSION CPPCH4(30),YKCH4(30),VICH4(30)
C
C     DOUBLE PRECISION PARAMETERS THAT CHANGE SLOWLY DUE TO
C     CARBON DEPOSITION
       DOUBLE PRECISION PRESS,PRSX,TPRSX,RN,WI,GTH
       DOUBLE PRECISION PRSS
C
C     OPEN DATA FILES FOR PHYSICAL PROPERTIES
C       SPECIFIC HEAT
       OPEN(UNIT=1,FILE='CPCO2.DAT',STATUS='OLD')
       OPEN(UNIT=2,FILE='CPCH4.DAT',STATUS='OLD')
C      GAS THERMAL CONDUCTIVITY
       OPEN(UNIT=3,FILE='KCO2.DAT',STATUS='OLD')
       OPEN(UNIT=4,FILE='KCH4.DAT',STATUS='OLD')
C      VISCOSITY
       OPEN(UNIT=7,FILE='VCO2.DAT',STATUS='OLD')
       OPEN(UNIT=8,FILE='VCH4.DAT',STATUS='OLD')
C      SOLID THERMAL CONDUCTIVITY
       OPEN(UNIT=10,FILE='KC.DAT',STATUS='OLD')
       OPEN(UNIT=11,FILE='KP.DAT',STATUS='OLD')
C     OPEN A DATA FILE FOR PROGRAM OUTPUT
       OPEN(UNIT=12,FILE='HDATA',STATUS='NEW')
C
C     READ IN THE SIZE OF THE PHYSICAL PROPERTY FILES
       READ(1,*)NTB1
       READ(2,*)NTB2
       READ(3,*)NTB3
       READ(4,*)NTB4
       READ(7,*)NTB7
       READ(8,*)NTB8
```

```
      READ(10,*)NTB10
      READ(11,*)NTB11
C
C     READ IN DATA FROM THE PHYSICAL PROPERTY FILES
      READ(1,*)(TCO2(II),CPPCO2(II),II=1,NTB1)
      READ(2,*)(TCH4(II),CPPCH4(II),II=1,NTB2)
      READ(3,*)(TCO22(II),YKCO2(II),II=1,NTB3)
      READ(4,*)(TCH42(II),YKCH4(II),II=1,NTB4)
      READ(7,*)(TCO23(II),VICO2(II),II=1,NTB7)
      READ(8,*)(TCH43(II),VICH4(II),II=1,NTB8)
      READ(10,*)(TC(II),CA(II),II=1,NTB10)
      READ(11,*)(TP(II),PK(II),II=1,NTB11)
C
C     SET THE NUMBER OF HEAT EXCHANGER SECTIONS
      STEP=999.
      ISTEP=999
C     ENTER IN DIMENSIONS OF THE EXCHANGER CHANNEL
      R=0.00025
      PI=3.141592654
      PIH=PI/2.0
      WI=0.0005
      GTH=0.00102
C
C     SET THE VALUE FOR THE EFFECTIVE PLATINUM CROSS
C      SECTIONAL AREA
      AM=0.00497
C     SET THE VALUE FOR THE MOLAR DEPOSITION FRACTION
      GAMDEP=6.758E-08
C
C     INPUT THE OPERATING PARAMETERS FOR THE HEAT EXCHANGER
      WRITE(6,10)
   10 FORMAT(' INPUT TYPE OF GAS TO BE USED')
      WRITE(6,20)
   20 FORMAT(' CO2=1, CH4=2')
      READ(6,30)J
   30 FORMAT(I2)
C     SET THE GAS CONSTANT
      IF(J.EQ.1)THEN
          RG=188.955
        ELSE
        IF(J EQ.2)THEN
            RG=518.390
          ELSE
          ENDIF
        ENDIF
   50 FORMAT(I3)
      WRITE(6,60)
   60 FORMAT(' INPUT LENGTH OF TEST (HRS)')
      READ(6,70)ITIME
   70 FORMAT(I5)
C     COMPUTE CHANNEL STEP SIZE
      DX=0.102/STEP
```

```
      WRITE(6,80)
   80 FORMAT(' INPUT TOTAL MASS FLOW RATE (KG/HR):')
      READ(6,90)TMF
   90 FORMAT(F6.5)
C    CONVERT TOTAL MASS FLOW RATE INTO CHANNEL MASS
C     FLOW RATE
C    IN KG/SEC
      FM=TMF/129600.0
      WRITE(6,100)
  100 FORMAT(' INPUT INLET PRESSURE (ATM):')
      READ(6,110)PATM
  110 FORMAT(F3.2)
      WRITE(6,120)
  120 FORMAT(' INPUT APPROX. INLET TEMP. (K):')
      READ(6,130)TGUES
  130 FORMAT(F7.2)
      WRITE(6,140)
  140 FORMAT(' INPUT UNIT POWER (W)')
      READ(6,150)QENT
  150 FORMAT(F10.4)
C
C    CONVERT UNIT POWER INTO THE FRACTIONAL POWER FOR EACH
C    CHANNEL SECTION
      Q=(QENT*0.663)/(STEP*36)
C
C    SET EXCHANGER INLET VALUES FOR
      DO 160 I=1,ITIME
C    TEMPERATURE
      TM(1,I)=298.0
      TM(2,I)=298.0
C    CROSS SECTIONAL AREA
      A(1,I)=6.08175E-07
  160 CONTINUE
C    LATERAL HEAT FLUX
      QD(1)=0.
      QD(2)=0.
C
C    ANALYZE EXCHANGER FOR A TIME INCREMENT
      DO 300 IT=1,ITIME
      PRSS=PATM*101325.
      RHO=(RG*TM(1,IT))/PRSS
C    GUESS THE INLET SURFACE TEMPERATURE
      TI=TGUES
  170 TS(1)=TI
      TS(2)=TI
C    RESET PRESSURE AND RADICAL CONCENTRATION COUNTERS
      TPRSX=0.
      CONC=0.
C
      DO 200 IL=2,ISTEP+1
C    ANALYZE A SECTION OF THE HEAT EXCHANGER
      PRESS=PRSS
```

```
C     DETERMINE VALUES FOR THE GAS PHYSICAL PROPERTIES AT
C      THIS SECTION AND TIME
        IF(J.EQ.1)THEN
            CALL TBLOOK(TM(IL,IT),NTB1,TCO2,CPPCO2,CP)
            CALL TBLOOK(TM(IL,IT),NTB3,TCO22,YKCO2,GK)
            CALL TBLOOK(TM(IL,IT),NTB7,TCO23,VICO2,VIS)
          ELSE
          IF(J.EQ.2)THEN
              CALL TBLOOK(TM(IL,IT),NTB2,TCH4,CPPCH4,CP)
              CALL TBLOOK(TM(IL,IT),NTB4,TCH42,YKCH4,GK)
              CALL TBLOOK(TM(IL,IT),NTB8,TCH43,VICH4,VIS)
            ELSE
          ENDIF
        ENDIF
C     DETERMINE SOLID PHYSICAL PROPERTIES
        CALL TBLOOK(TS(IL),NTB11,TP,PK,PKK)
        CALL TBLOOK(TS(IL),NTB10,TC,CA,CK)
C
C     CORRECT CHANNEL DIMENSIONS FOR CARBON DEPOSITION
        RN(IL)=R-DEP(IL,IT)
        DPT(IL)=2.0*DEP(IL,IT)
C     CROSS SECTIONAL AREA
        A(IL,IT)=(PIH*(RN(IL)**2.0))+((WI-DPT(IL))*
      C(GTH-DEP(IL,IT)))
C     CROSS SECTIONAL PERIMETER
        P(IL,IT)=(PI*RN(IL))+(WI-DPT(IL))+(2.0*
      C(GTH-DEP(IL,IT)))
C
C     COMPUTE HYDRAULIC RADIUS
        DH=(4.0*A(IL,IT))/P(IL,IT)
C     REYNOLDS NUMBER
        REY=(FM*DH)/(A(IL,IT)*VIS)
C     PRANDTL NUMBER
        PR=(CP*VIS)/GK
C     COEFFICIENT OF HEAT TRANSFER
        H(IL)=(4.5*GK)/DH
C
C     COMPUTE TEMPERATURE INCREASE IN THE SECTION
        DTMT=(H(IL)*(CK*P(IL,IT)))*(DX*(TS(IL)-TM(IL,IT)))
        DTMB1=CK+(DEP(IL,IT)*H(IL))
        DTMB=DTMB1*(FM*CP)
        DTM=DTMT/DTMB
C
C     CHECK IF TURBULENT FLOW TRANSITION LIMIT IS MET
        IF(REY.LE.2100.)THEN
          ELSE
            WRITE(6,180)IT
  180       FORMAT(' TURBULENT FLOW REACHED AT T=',I5,'HRS')
            GOTO 310
          ENDIF
C
C     COMPUTE ADJUSTED PRESSURE FOR THIS SECTION
        FF=16.43/REY
```

```
          PRSXT=((FF*DX)*(RG*TM(IL,IT)))*(FM**2.)
          PRSXB=(DH*PRESS)*(A(IL,IT)**2.)
          PRSX=PRSXT/PRSXB
          TPRSX=TPRSX+PRSX
          PRESS=PRSS-TPRSX
C
C     COMPUTE NEW DEPOSITION RATE
          IF(J.EQ.2)THEN
C         CONVERT PRESSURE TO ATM
              PRESA=PRESS/101325.
C         COMPUTE KINETIC RATE EQUATION
              RATE=(25.*PRESA)*EXP(-8153./TM(IL,IT))
C         COMPUTE SECTION TRAVEL TIME
              TRES=((DX*A(IL,IT))*PRESS)/((FM*RG)*TM(IL,IT))
C         CHANGE IN RADICAL CONCENTRATION
              CONCP=RATE*TRES
C         NEW RADICAL CONCENTRATION
              CONC=CONC+CONCP
C         MEAN RADICAL MOLECULAR VELOCITY
              CBAR=47.014*(TM(IL,IT)**0.5)
C         MOLAR FLUX
              TFLUX=(250.*CONC)*CBAR
C         DEPOSITION INCREASE FOR THIS TIME INCREMENT
              DEPN=(GAMDEP*TFLUX)/45.0976
C         COMPUTE DEPOSITION THICKNESS FOR NEXT TIME INCREMENT
              DEP(IL,IT+1)=DEP(IL,IT)+DEPN
            ELSE
          ENDIF
C
C     COMPUTE FLUID TEMPERATURE FOR NEXT SECTION
          TM(IL+1,IT)=TM(IL,IT)+DTM
C
C     COMPUTE SURFACE TEMPERATURE FOR NEXT SECTION
C      HEAT FLUX TO FLUID
          QF=DTMT/DTMB1
C      ENERGY BALANCE FOR SECTION
C        TO FIND LATERAL HEAT FLUX TO NEXT SECTION
          QD(IL+1)=(QF+QD(IL))-Q
C     COMPUTE INCREASE IN SURFACE TEMPERATURE
          DQTF=(QD(IL+1)*DX)/(PKK*AM)
C     COMPUTE NEXT SECTION SURFACE TEMPERATURE
          TS(IL+1)=((2.*TS(IL))-TS(IL-1))+DQTF
C
C     GO ON TO NEXT SECTION
  200   CONTINUE
C
C     CHECK THAT LATERAL HEAT FLUX AT LAST SECTION
C        IS NEAR ZERO
          QABS=ABS(QD(ISTEP+1))
          IF(QABS.GE.0.004)THEN
```

```
C     IF HEAT FLUX IDS TOO LARGE, CORRECT GUESS FOR
C        CHANNEL INLET SURFACE TEMPERATURE
            IF(QD(ISTEP+1).LT.0.)THEN
                TI=TI+0.2
              ELSE
                TI=TI-0.2
              ENDIF
C     INSERT A COUNTER TO LIMIT THE NUMBER OF TEMPERATURE
C          ITERATIONS
             JJ=JJ+1
             IF(JJ.GE.600)THEN
                 WRITE(6,210)
  210            FORMAT(' TOO MANY ITERATIONS')
                 WRITE(6,220)QD(ISTEP+1)
  220            FORMAT(' QD=',F10.6)
C     IF THERE ARE TOO MANY ITERATIONS, CUT OFF PROGRAM
                 GOTO 310
               ELSE
               ENDIF
C     RETURN TO CHANNEL INLET WITH NEW TEMPERATURE GUESS
           GOTO 170
         ELSE
C     IF END LATERAL HEAT FLUX IS OK, CONTINUE ON
          ENDIF
C     RESET COUNTER
        JJ=1
C
C     MOVE TO NEXT TIME INCREMENT
  300   CONTINUE
C
C     ANALYSIS IS COMPLETE
C       MOVE TO DATA OUTPUT
C
C     THIS SECTION MAY BE MODIFIED TO DISPLAY WHATEVER
C        OUTPUT IS REQUIRED
  310   CONTINUE
C
C     USE OUTPUT FILE TO COLLECT DEPOSITION DATA
  320   DO 350 IM=2,ISTEP+1,15
        XINC=IM-1.
        XLOC=(XINC/STEP)*10.2
C     CONVERT DEPOSITION FROM M TO MICRONS
        DEPMIC=DEP(IM,ITIME)*1.0E06
        WRITE(12,*)XLOC,DEPMIC
  350   CONTINUE
        XLOC=10.2
        DEPMIC=DEP(ISTEP+1,ITIME)*1.0E06
        WRITE(12,*)XLOC,DEPMIC
        WRITE(6,410)DEPMIC
  410   FORMAT(' EXIT DEPOSITION=',F10.5,' MICRONS')
        WRITE(6,420)TI
  420   FORMAT(' INLET SURFACE TEMP= ',F10.3)
        PRESA=PRESS/101325.
```

```
      WRITE(6,430)TM(ISTEP+1,ITIME),TS(ISTEP+1)
  430 FORMAT(' CHAMBER TEMP=',F9.3,' OUTLET SURFACE T=',
     CF9.3)
      WRITE(6,440)PRESA
  440 FORMAT(' EXIT PRESSURE=',F6.4,' ATM')
      STOP
      END


      SUBROUTINE TBLOOK(T,NTABLE,TCO2,CPPCO2,CP)
C     THIS SUBROUTINE TAKES A GIVEN TEMPERATURE AND THE TABLE
C       DATA FOR A PROPERTY AND LINEARLY INTERPOLATES A
C       DESIRED PHYSICAL PROPERTY
      DIMENSION TCO2(NTABLE),CPPCO2(NTABLE)
      IF(T.GE.TCO2(1).AND.T.LE.TCO2(NTABLE))THEN
          DO 1110 NEXT=2,NTABLE
          IF(T.LE.TCO2(NEXT))THEN
              GOTO 1150
            ELSE
            ENDIF
 1110       CONTINUE
        ELSE
        ENDIF
      IF(T.LE.TCO2(1))THEN
          CP=CPPCO2(1)
        ELSE
          CP=CPPCO2(NTABLE)
        ENDIF
      WRITE(6,1120)T
 1120 FORMAT(' OUT OF TABLE RANGE AT T=',F10.5)
      STOP
 1150 CONTINUE
      B=(T-TCO2(NEXT-1))*(CPPCO2(NEXT)-CPPCO2(NEXT-1))
      IF(TCO2(NEXT).EQ.TCO2(NEXT-1))THEN
          WRITE(6,1155)T,CP
 1155       FORMAT(' T=',F10.5,' CP=',F10.5)
          STOP
        ELSE
        ENDIF
      CP=(B/(TCO2(NEXT)-TCO2(NEXT-1)))+CPPCO2(NEXT-1)
 1160 CONTINUE
      RETURN
      END
```

Bibliography

1. Bird, R. Byron et al. Transport Phenomena. New York: John Wiley & Sons, Inc., 1960.

2. Bowman, George P., Jr. "Thermochemistry (Propulsion Applications)." Lecture Notes. School of Engineering, Air Force Institute of Technology (AU), Wright-Patterson AFB OH, March 1965.

3. Braunscheidel, Edward P. "Performance Characterization and Transient Investigation of Multipropellant Resistojets," AIAA Paper 89-2837. Washington, D.C.: AIAA, 1989.

4. Breyley, Loranell et al. "Effect of Nozzle Geometry on the Resistojet Exhaust Plume," AIAA Paper 87-2121. Washington, D.C.: AIAA, 1987.

5. Chen, C. J. et al. "Mechanism of the Thermal Decomposition of Methane," Industrial and Laboratory Pyrolyses, ACS Symposium Series 32, edited by Lyle F. Albright and Billy L. Crynes. Washington, D.C.: American Chemical Society, 1976.

6. Chou, Mau-Song. "Multiphoton Ionization of Methyl Radicals in CH_4 Pyrolysis," Chemical Physics Letters, 114: 279-281 (March 1985).

7. Haaland, Peter D., Associate Professor. Personal interviews. Air Force Institute of Technology, Wright-Patterson AFB OH, 1 October 1989 through 23 January 1990.

8. Happel, John and Leonard Kramer. "Acetylene and Hydrogen from the Pyrolysis of Methane," Industrial and Engineering Chemistry, 59: 39-50 (January 1967).

9. Heckert, Bruce J. Space Station Resistojet System Requirements and Interface Definition Study, Contract NAS3-24658. Canoga Park CA: Rocketdyne Division, Rockwell International Corperation, February 1987 (NASA-CR-179581).

10. Hirt, T. J. and H. B. Palmer. "Kinetics of Deposition of Pyrolitic Carbon Films from Methane and Carbon Suboxide," Carbon, 1: 65-70 (1963).

11. Ho, C. Y. et al. "Thermal Conductivity of the Elements," Journal of Physical and Chemical Reference Data, 1: 279-420 (February 1972).

12. Incropera, Frank P. and David P. Dewitt. Introduction to Heat Transfer. New York: John Wiley & Sons, Inc., 1985.

13. Jones, Robert E. "High and Low Thrust Propulsion Systems for the Space Station," AIAA Paper 87-0398. Washington, D.C.: AIAA, 1987.

14. Khan, M. S. and Billy L. Crynes. "Survey of Recent Methane Pyrolysis Literature," Industrial and Engineering Chemistry, 62: 54-59 (October 1970).

15. Kozlov, G.I. and V. G. Knorre. "Single-Pulse Shock Tube Studies on the Kinetics of the Thermal Decomposition of Methane," Combustion and Flame, 6: 253-263 (December 1962).

16. Laidler, Keith J. Chemical Kinetics. New York: McGraw-Hill Book Company, 1965.

17. Lieske, Heiner et al. "Hydrocarbon Adsorption and Coke Formation on Pt/Al_2O_3 and $Pt-Sn/Al_2O_3$ Catalysts," Applied Catalysis, 30: 69-80 (1987).

18. Morren, W. Earl et al. "Performance Characterizations of an Engineering Model Multipropellant Resistojet," Journal of Propulsion and Power, 5: 197-203 (March-April 1989).

19. National Aeronautics and Space Administration. Resistojet Design Review Plans. Cleveland: NASA Lewis Research Center, 25 February 1987.

20. National Bureau of Standards. JANAF Thermochemical Tables (Second Edition). NSRDS-NBS 37. Washington, D.C.: Office of Standard Reference Data, June 1971.

21. Palmer, H. B. et al. "On the Kinetics and Mechanism of the Thermal Decomposition of Methane in a Flow System," The Journal of Physical Chemistry 72: 348-353 (January 1968).

22. Palmer, Howard B. and Thomas J. Hirt. "The Activation Energy for the Pyrolysis of Methane," The Journal of Physical Chemistry, 67: 709-711 (March 1963).

23. Phillips, D. G. Technology Development of a Biowaste Resistojet, Volume 1, Contract NAS 1-9474. Van Nuys, CA: The Marquardt Company, June 1972 (NASA-CR-112149).

24. Phillips, D. G. Technology Development of a Biowaste Resistojet, Volume 2, Contract NAS 1-9474. Van Nuys, CA: The Marquardt Company, June 1972 (NASA-CR-112150).

25. Planeaux, James B. Lecture Notes for MENG 632, Nonchemical Rocket Propulsion. School of Engineering, Air Force Institute of Technology (AU), Wright-Patterson AFB OH, April 1989.

26. Pugmire, T. K. et al. "A 10,000 Hour Life Multipropellant Engine for Space Station Applications," AIAA Paper 86-1403. Washington, D.C.: AIAA, 1986.

27. Rohsenow, Warren M. and James P. Hartnett. Handbook of Heat Transfer. New York: McGraw-Hill Book Company, 1973.

28. Shah, Ramesh K. "Fully Developed Laminar Flow Forced Convection in Channels," Low Reynolds Number Flow Heat Exchangers, edited by Sadik Kakaç et al. Washington, D.C.: Hemisphere Publishing Company, 1983.

29. Sutton, George P. Rocket Propulsion Elements (Fifth Edition). New York: John Wiley & Sons, Inc., 1986.

30. Touloukian, Y. S. et al. Thermophysical Properties of Matter, Volume 3: Thermal Conductivity, Nonmetallic Liquids and Gases. New York: IFI/Plenum Data Corporation, 1970.

31. Wang, Po-Kang et al. "Observation of Isolated Carbon Atoms and the Study of Their Mobility on Pt Clusters by NMR," Physical Review Letters, 55: 2731-2734 (December 1985).

32. Whalen, Margaret V. and Stanley P. Grisnik. "Compatibility of Grain-Stabilized Platinum With Candidate Propellants for Resistojets," AIAA Paper 85-2014. Washington, D.C.: AIAA, 1985.

33. Younglove, B. A. and J. F. Ely. "Thermophysical Properties of Fluids: II. Methane, Ethane, Propane, Isobutane, and Normal Butane," Journal of Physical and Chemical Reference Data, 16: 577-794 (July-August 1987).

VITA

Captain John A. Vise [redacted]. He graduated from Aurora Central High School in Aurora, Colorado in 1979. He received the degree of Bachelor of Science in Civil Engineering from the University of Colorado in December, 1983, and was commissioned in the USAF through the ROTC program. His first assignment was to the 4th Civil Engineering Squadron, Seymour Johnson AFB, NC, where he served as a design engineer, and as Deputy Chief of Contract Management. During the summer of 1987, he performed temporary duty as a design engineer for Southern Command Joint Task Force Bravo, Palmerola AB, Honduras. Captain Vise entered the School of Engineering, Air Force Institute of Technology, in June 1988. He has been registered as a Professional Engineer in North Carolina since 1988.

[redacted]

REPORT DOCUMENTATION PAGE

Form Approved OMB No. 0704-0188

1a. REPORT SECURITY CLASSIFICATION: UNCLASSIFIED

1b. RESTRICTIVE MARKINGS:

2a. SECURITY CLASSIFICATION AUTHORITY:

2b. DECLASSIFICATION / DOWNGRADING SCHEDULE:

3. DISTRIBUTION / AVAILABILITY OF REPORT: Approved for public release; distribution unlimited

4. PERFORMING ORGANIZATION REPORT NUMBER(S): AFIT/GA/ENY/90M-2

5. MONITORING ORGANIZATION REPORT NUMBER(S):

6a. NAME OF PERFORMING ORGANIZATION: School of Engineering

6b. OFFICE SYMBOL (If applicable): AFIT/EN

7a. NAME OF MONITORING ORGANIZATION:

6c. ADDRESS (City, State, and ZIP Code): Air Force Institute of Technology (AU)
Wright-Patterson AFB, Ohio 45433-6583

7b. ADDRESS (City, State, and ZIP Code):

8a. NAME OF FUNDING / SPONSORING ORGANIZATION:

8b. OFFICE SYMBOL (If applicable):

9. PROCUREMENT INSTRUMENT IDENTIFICATION NUMBER:

8c. ADDRESS (City, State, and ZIP Code):

10. SOURCE OF FUNDING NUMBERS

PROGRAM ELEMENT NO.	PROJECT NO.	TASK NO	WORK UNIT ACCESSION NO.

11. TITLE (Include Security Classification): ANALYSIS OF THE USE OF A METHANE PROPELLANT IN A BIOWASTE RESISTOJET

12. PERSONAL AUTHOR(S): John A. Vise, Captain, USAF

13a. TYPE OF REPORT	13b. TIME COVERED	14. DATE OF REPORT (Year, Month, Day)	15. PAGE COUNT
MS Thesis	FROM _____ TO _____	1990 March	118

16. SUPPLEMENTARY NOTATION:

17. COSATI CODES		
FIELD	GROUP	SUB-GROUP
21	03	

18. SUBJECT TERMS (Continue on reverse if necessary and identify by block number): Electric Propulsion; Resistojets; Methane; Space Station; Nonchemical Propellants

19. ABSTRACT (Continue on reverse if necessary and identify by block number)

see reverse

Title: Analysis of the Use of a Methane Propellant in a Biowaste Resistojet

Advisor: Captain James B. Planeaux, PhD
Associate Professor
Department of Aeronautics and Astronautics

20. DISTRIBUTION / AVAILABILITY OF ABSTRACT
☒ UNCLASSIFIED/UNLIMITED ☐ SAME AS RPT. ☐ DTIC USERS

21. ABSTRACT SECURITY CLASSIFICATION: UNCLASSIFIED

22a. NAME OF RESPONSIBLE INDIVIDUAL: Capt. James B. Planeaux, USAF

22b. TELEPHONE (Include Area Code): 513-255-3517

22c. OFFICE SYMBOL: AFIT/ENY

DD Form 1473, JUN 86 — Previous editions are obsolete.